Developmental Biology **249,** 300–320 (2002)
doi:10.1006/dbio.2002.0771

in the Forelimb of the Quail Embryo

Damien Bates,*,†,[1] G. Ian Taylor,† and Donald F. Newgreen*

**Embryology Laboratory, MCRI, Royal Children's Hospital, Flemington Road, Parkville, Victoria 3052, Australia; and †Plastic and Reconstructive Surgery Research Unit, Royal Melbourne Hospital, 766 Elizabeth Street, Melbourne, Victoria 3000, Australia*

Peripheral nerve and vascular patterns are congruent in the adult vertebrate, but this has been disputed in vertebrate embryos. The most detailed of these studies have used the avian forelimb as a model system, yet neurovascular anatomical relationships and critical vascular remodeling events remain inadequately characterized in this model. To address this, we have used a combination of intravascular marker injection, multilabel fluorescent stereomicroscopy, and confocal microscopy to analyze the spatiotemporal relationships between peripheral nerves and blood vessels in the forelimb of 818 quail embryos from E2 (HH13) to E15 (HH41). We find that the neurovascular anatomical relationships established during development are highly stereotypic and congruent. Blood vessels typically arise before their corresponding nerves, but there are several critical exceptions to this rule. The vascular pattern is extensively remodeled from the earliest stage examined (E2; HH13), whereas the peripheral nerves, the first of which enter the forelimb at E3.5–E4 (HH21–HH24), have a progressively unfolding pattern that, once formed, remains essentially unchanged. The adult neurovascular pattern is not established until E8 (HH34). Peripheral nerves are always found to track close and parallel to the vasculature. As they track distally, peripheral nerves always lie on the side of the vasculature away from the center of the forelimb. Neurovascular patterns have a hierarchy of congruence that is highest in the dorsoventral plane, followed by the anteroposterior, and lastly the proximodistal planes.

Key Words: **neurovascular; nerves; blood vessels; endothelium; patterning; quail; forelimb; median artery.**

INTRODUCTION

The close spatial relationship between peripheral nerves and blood vessels in the adult vertebrate is well documented (Taylor *et al.*, 1994). Neurovascular associations have also been described in wound healing (Gu *et al.*, 1994, 1995; Kangesu *et al.*, 1998; Manek *et al.*, 1993; Waris, 1978a,b), nerve regeneration (Hobson *et al.*, 1997, 2000; Ramer *et al.*, 2000), and neoplasia (Jang *et al.*, 2000). Neurovascular congruence must arise during embryonic development, and understanding its molecular bases would be of great importance to embryological research. Equally, such an understanding would have profound implications for reconstructive surgery and regenerative medicine (Tabata, 2001). However, the reality and generality of this neurovascular parallelism in embryos is still being disputed (Bennett *et al.*, 1980; Martin and Lewis, 1989; Piatt, 1942; Spence and Poole, 1994; Swanson and Lewis, 1982; Tello, 1917; Tosney and Landmesser, 1985). Obviously, the first goal toward understanding neurovascular relationships at a molecular level is to establish the reality of neurovascular congruence in an amenable model system by describing, in spatiotemporal detail, the developmental anatomy. At this point, in view of the increasing molecular evidence linking the development of nerves and blood vessels in the embryo (Roush, 1998; Shima and Mailhos, 2000), meaningful experimental studies could be initiated.

The avian limb is a classical model for analysis of vertebrate pattern formation (Tabin, 1991; Tickle, 1991) and has been used to analyze the peripheral nerve (Hollyday, 1995; Stirling and Summerbell, 1977; Swanson and Lewis, 1982) and vascular (Flamme *et al.*, 1995) pattern. Although there is as yet incomplete information on the vascular pattern (see below), the neural developmental pattern in the limb is described in detail (Hollyday, 1995; Roncali, 1970; Stirling and Summerbell, 1977; Swanson and Lewis, 1982). In addition, a major advantage of this system

[1] To whom correspondence should be addressed. Fax: (613) 93 48 1391. E-mail: bates_damien@hotmail.com.

0012-1606/02 $35.00

is its ability to be experimentally manipulated by ablation, recombination, bead implantation, viral infection, and electroporation (Weaver and Hogan, 2001). Studies describing the anatomical relationship between peripheral nerves and blood vessels in the limb of the developing embryo have been limited principally because their aim was not to analyze neurovascular pattern but to determine what was responsible for stereotypic nerve patterns (Bennett *et al.*, 1980; Martin *et al.*, 1989; Martin and Lewis, 1989; Spence and Poole, 1994; Tosney and Landmesser, 1985). Thus, in some studies, the vasculature was not labeled (Bennett *et al.*, 1980; Tosney and Landmesser, 1985) or was incompletely described; for example, Bennett *et al.* (1980) refer to only two capillary networks in the forelimb, where there are actually four (Seichert and Rychter, 1971, 1972a,b,c). Conclusions regarding the spatial relationships between nerves and blood vessels have been largely based on two-dimensional data obtained from histological sections at specific time points (Tosney and Landmesser, 1985). This simplifies the complex three-dimensional structure of a limb that changes with time (Bennett *et al.*, 1980). It is also well known that the vasculature is remodeled (Peng *et al.*, 2000), so it is possible that critical nerve–blood vessel relationships may have been overlooked because of their transience (Piatt, 1942). Similarly, conclusions that the peripheral nerve pattern is unrelated to the vascular pattern have been based on a few examples of lack of congruence between nerves and major blood vessels (e.g., subclavian artery) (Bennett *et al.*, 1980). It may be unjustified to extrapolate observations of specific, accessible examples (e.g., whole-mount preparations of dorsal wing skin) (Martin and Lewis, 1989) to neurovascular patterning in general.

The vascular anatomy of the adult avian forelimb has been well described (Nickel *et al.*, 1977), but detailed descriptions of the vascular remodeling that gives rise to this adult pattern are incomplete (Caplan, 1985; Caplan and Koutroupas, 1973; Drushel *et al.*, 1985; Feinberg *et al.*, 1986). The developmental anatomy of the major blood vessels has only been described in detail to E4.5 (HH25) (Caplan and Koutroupas, 1973; Coffin and Poole, 1988; Drushel *et al.*, 1985; Evans, 1909; Feinberg *et al.*, 1986). Descriptions of vascular anatomy beyond E4.5 are limited to the capillaries and peripheral venous system, rather than the arteries which supply them (Seichert and Rychter, 1971, 1972a,b,c).

In view of the importance of neurovascular relationships and their incomplete description in an experimentally amenable developmental system, we have examined in detail the spatiotemporal relationship of peripheral nerves and blood vessels in the forelimb of the quail embryo. We find that the development of neurovascular pattern is more complex than previously appreciated, and the mode of development of peripheral nerves and blood vessels is different. Nerves project progressively and then remain relatively static (Hollyday, 1990). The vasculature, on the other hand, is dynamic with a changing pattern (Evans, 1909). Despite these differences, the pattern of neurovascular development is highly stereotypic and congruent. In general, blood vessels form discrete patterns prior to peripheral nerve in-growth, which gives the impression that nerves follow the vasculature. However, there are several examples where nerves precede the in-growth and foreshadow the trajectory of their corresponding arteries. In situations where a peripheral nerve is not associated with a major blood vessel in the anteroposterior (A-P) plane, it is invariably found to lie on one of four capillary layers in the dorsoventral (D-V) plane. These capillary layers are related to (but do not appear to be defined by) the avascular cartilage in the center of the forelimb, the dorsal and ventral muscle masses, and the subectodermal avascular zone. Peripheral nerves maintain a characteristic position in relation to the blood vessels with which they track. This is always on the side of the vasculature away from the geometric center of the forelimb. Finally, neurovascular patterns have a hierarchy of congruence. Congruence is highest in the D-V plane, followed by the A-P and proximodistal (P-D) planes.

MATERIALS AND METHODS

Quail Microinjection Methods

Quail embryos (*Coturnix coturnix japonica*) were obtained from Lago Game (Melbourne, Australia) and incubated at 38°C to defined stages (Hamburger and Hamilton, 1951) between E2 (HH13) and E15 (HH41).

Micropipettes (50 μl; Fisher Scientific, NH) were manually pulled over a flame to a diameter of 5–20 μm. India Ink (Pelikan No. 17 Black; Pol Equipment, Sydney, Australia) was diluted 1:1 in PBS and centrifuged at 4000 rpm for 1 min, and the supernatant was warmed to 38°C prior to injection. The solution of India Ink was injected into the embryo as previously described (Caplan and Koutroupas, 1973; Evans, 1909; Seichert and Rychter 1971, 1972a,b,c). Embryos that were not perfused completely were discarded. Embryos were also perfused with fluorescent dyes for double-labeling confocal analysis. Both TRITC-conjugated high mw dextran (undiluted, D-7139; Molecular Probes, OR) and SP-DiI (4 mg/ml DMSO, D-7777; Molecular Probes) diluted 1/16 in PBS were used.

Whole-Mount Immunolabeling

Perfused embryos were immediately fixed in 4% paraformaldehyde (PFA) and kept overnight at 4°C. Embryos were then washed three times in PBS before the forelimbs were dissected from the rest of the embryo. Embryos of E7 (HH32) and older had the dorsal or ventral ectoderm removed to facilitate antibody penetration. Dorsal and ventral cutaneous nerves were analyzed in those specimens in which the ectoderm was retained. Whole forelimbs were blocked with 1% bovine serum albumin (BSA; Roche, Sydney, Australia) for 1 h at room temperature on a rocker. All antibodies were prepared in 1% BSA and 0.1% Triton X-100 (BDH Laboratory Supplies, UK). Nerves were labeled with TUJ1 (BabCO, Chemicon, Melbourne, Australia) diluted 1/250 overnight at 4°C on a rocker. Forelimbs were then washed three times in PBS (5 min each wash) after which goat anti-Mouse IgG Alexa 488 (Molecular Probes) secondary antibody diluted 1/100 was applied and left overnight at 4°C on a

rocker. Forelimbs were again washed three times in PBS before being cleared in a series of increasing concentrations of glycerol (BDH Laboratory Supplies, UK) in PBS. Forelimbs were then left in 90% glycerol overnight before being visualized in whole mount.

Image Orientation, Sectioning, and Capture

Whole-mount forelimbs were transferred to a 3-cm petri dish in 90% glycerol for image analysis. Forelimbs were also cut freehand into thick (50–300 μm) sections by using a sapphire microscalpel (World Precision Instruments, Melbourne, Australia). Standard sections were coronal (perpendicular to the P-D and A-P forelimb axes) and sagittal (perpendicular to the D-V and A-P forelimb axes). Whole-mount and sectioned forelimbs were visualized with the Leica MZ FL III (Leica Microsystems, Switzerland) fluorescent stereomicroscope. Images were captured with a Leica DC200 digital camera III (Leica Microsystems, Switzerland) and processed with proprietary Leica IM1000 software (Ver 1.10 Release 17). Images were captured as 1798 × 1438-pixel JPEG files. Either brightfield, GFP3 fluorescent filter images, or typically both (for double labeling) were obtained with the specimen in the same orientation and at the same magnification. The *gamma* function of the Leica software was manipulated to reveal the India Ink-labeled blood vessels with the GFP3 fluorescent filter enabling simultaneous analysis of the three-dimensional neurovascular anatomical relationships.

Image Analysis

JPEG files were subsequently opened in Adobe Photoshop 5.0 (v5.0.2; Adobe Systems Inc., CA). Brightfield images were overlaid with their Alexa 488 counterparts by using the Photoshop *Layer* function. Precise positioning of the overlaid image was achieved by using a series of blood vessels in both images as fiduciary points.

Confocal Imaging Techniques

The confocal technique has been described in detail elsewhere (Taylor *et al.*, 2001). Briefly, whole-mount forelimbs were scanned at 8-μm intervals in the transverse plane of the forelimb with the ×10 objective of the confocal microscope (Bio-Rad MRC1024, mounted on a Zeiss Axioskop fluorescence microscope, with a Krypton/Argon laser; Bio-Rad Laboratories, Sydney, Australia). Alexa 488 and TRITC images were recorded simultaneously and merged by using Bio-Rad proprietary software (Bio-Rad Laboratories, Sydney, Australia).

Frozen Sections

Forelimbs were fixed in 4% PFA overnight at 4°C, washed three times in PBS, then placed overnight in 30% sucrose in PBS at 4°C. Forelimbs were then transferred to Tissue Tek cryomolds (Miles Inc., IN) and oriented in TBS Tissue Freezing Medium (ProSciTech, Thuringowa, Australia). Then, 20-μm sections were cut in either the coronal or the sagittal plane. Sections were placed on poly-L-lysine-coated Superfrost PLUS microscope slides (Biolab Scientific, Auckland, NZ) and allowed to dry overnight at room temperature. Sections were pretreated for 10 min with 100 μl 1% BSA prior to application of the primary and secondary antibodies. Blood vessels were labeled with QH-1 (Developmental Hybridoma Bank, IO) at 1/50 dilution. Peripheral nerves were labeled with 1/200 rabbit anti-Neurofilament M C-terminal polyclonal antibody (AB1987; Chemicon Intl., Melbourne, Australia). Both antibodies were prepared in 1% BSA and 0.1% Triton X-100. Goat anti-mouse IgG Alexa 546 (1/400; Molecular Probes) and goat anti-rabbit IgG Alexa 488 (1/400; Molecular Probes) were used as secondary antibodies. Sections were exposed to the primary antibodies under a coverslip overnight at 4°C and then washed three times in PBS. The secondary antibodies were then applied and also left overnight at 4°C under a coverslip. After an additional three washes in PBS and draining, sections were mounted in Fluoroguard Antifade Reagent (Bio-Rad Laboratories). Image analysis was performed by using an Axioskop fluorescence microscope equipped with a ×20 objective (Carl Zeiss Inc., Sydney, Australia), a charge-coupled device camera (Photometrics Image Point, AZ), and IPLAB software (Signal Analytics, VA).

TABLE 1

Number of Quail Embryos Analyzed at Each Stage of Development

Stage	Fluorescent stereomicroscopy[a]	Confocal microscopy[a]
E2 (HH13)	13	4
E2.5–E3 (HH17–HH20)	20	4
E3.5–E4 (HH22–HH24)	28	12
E4.5 (HH25)	61	8
E5 (HH26)	137	8
E5.5 (HH27–HH28)	238	5
E6.0 (HH29)	102	7
E6.5 (HH30)	76	8
E7 (HH32)	29	5
E8 (HH34)	28	0
E9–E10 (HH35–HH36)	15	0
E15 (HH41)	10	0
Total	757 (1514 forelimbs)	61 (122 forelimbs)

[a] The numbers below the heading in each column refer to the total number of embryos analyzed at each stage of development. In each embryo, the neurovascular pattern was analyzed in both forelimbs. Only morphologically normal embryos that were perfused and immunolabeled completely were included in this study.

RESULTS

General

A total of 1636 whole-mount forelimbs in 818 embryos aged between E2 and E15 (HH13–HH41) were analyzed in this study (Table 1). The neurovascular pattern obtained by frozen section immunolabeling of peripheral nerves and blood vessels was compared with the neurovascular pattern observed with both whole-mount fluorescent stereomicroscopy and confocal microscopy. The neurovascular patterns were similar in each of the methods used (data not shown). Fluorescent stereomicroscopy proved superior to confocal microscopy for visualization of neurovascular anatomy in whole-mount specimens older than E3 (HH20), particularly in the D-V plane. TUJ1 and anti-neurofilament antibodies produced equivalent peripheral nerve labeling patterns.

India Ink was superior to both QH-1 immunolabeling and fluorescent dye labeling for visualizing the complete forelimb vascular anatomy. In particular, the four discrete capillary layers (labeled I–IV in D-V order), along which peripheral nerves track, were better visualized when perfused with India Ink.

E2 (HH13–HH14)

Prior to HH13, dorsal aorta (DA) and posterior cardinal vein (PCV) formation has occurred (Coffin and Poole, 1988); however, capillary plexus down-growth from the Duct of Cuvier has not yet reached the lateral mesoderm opposite somites 15–20 that will later give rise to the forelimb (Chaube, 1959). There are also no branches from the DA projecting into this region at HH13 (Evans, 1909). Similarly, neural crest cells and motor axons have not yet migrated from the neural tube at the level of the prospective forelimb but by HH14, crest cells and axons are emerging from the neural tube opposite the anterior border of the forelimbs (Hollyday, 1983; Teillet and Le Douarin, 1983).

E2.5–E3 (HH17–HH20)

At HH17, a series of arteries branch from the lateral and dorsal surface of the DA (Evans, 1909). The lateral branches of the DA supplying the forelimb lie in both segmental and nonsegmental locations (Fig. 1A). The dorsal intersomitic artery (ISA) branches of the DA pass dorsomedially between adjacent somites in a strictly segmental manner to form a perineural capillary plexus on the lateral aspect of the neural tube. The intersomitic vein (ISV) drains the perineural capillary plexus. The ISV is a large vessel that is flattened anteroposteriorly (craniocaudally) and has a diameter of approximately 30 μm in the D-V plane (Fig. 1B). It drains directly into the PCV, which lies lateral and dorsal to the DA. Motor axons have emerged from the ventral aspect of the neural tube and contribute to the formation of forelimb spinal nerves in a distinct craniocaudal sequence. They pass laterally as a dorsoventrally flattened and loosely fasciculated sheet to the ventromedial portion of the somite. As they pass ventrolaterally, they are restricted to the anterior half of the somite, as are neural crest cells (Keynes and Stern, 1984). The most rostral axons within each spinal segment pass alongside the ventral half of the ISV (Fig. 1B). Axons did not appear to directly contact the blood vessels in the intersomitic cleft (ISA and ISV), but maintained a constant spatial relationship to them. This observation is consistent with that of Tosney and Landmesser (1985). Of all the axons which will later contribute to the formation of the spinal nerve, it is these most rostral axons (i.e., those positioned alongside the ISV) which have progressed farthest laterally. The lateral arterial branches of the DA supplying the forelimb pass ventral to the ISV and arch over the PCV to form a dense plexus of similarly sized capillaries in the ventral aspect of the forelimb (Figs. 1B and 1C). Motor axons continue to maintain their close spatial relationship to the ISV as they pass laterally and ventrally to the lateral edge of the somite at HH20. For this reason, the forelimb motor axons lie dorsal to the forelimb capillaries that branch from the DA in the region medial to the PCV. Lateral to the PCV, both axons and capillaries lie in the same D-V plane.

E3.5–E4 (HH21–HH24)

The forelimb blood vessel pattern is not static and undergoes significant remodeling during forelimb development. Those arteries, which arose from the lateral surface of the DA in nonsegmental positions, have now regressed. There are now multiple branches arising from the DA in strictly segmental positions (Evans, 1909). These branches no longer arise as a separate lateral branch from the DA, but arise from a common trunk with the ISA (Fig. 1D). This common arterial trunk is consistently located on the cranial side of the corresponding ISV (Spence and Poole, 1994). The ISA passes obliquely and ventromedially under the ISV toward the neural tube. Here, it joins the perineural capillary plexus on the caudal side of the ISV. The ISA also gives rise to capillary branches that form a vascular plexus surrounding each spinal nerve. Like the spinal nerves, this capillary plexus is restricted to the anterior half somite (data not shown). Further laterally, the neurovascular bundle between each somite is arranged so the arteries lie cranial to the veins and the veins lie cranial to their corresponding spinal nerves (Fig. 1D). In the D-V plane, however, nerves lie dorsal to arteries and arteries lie dorsal to veins.

The arterial branch of the DA passing to the forelimb in the space between the 18th and 19th somites has enlarged to become the largest artery supplying the forelimb (Fig. 1D). It is referred to as the primary subclavian artery (1°SCA) and is a direct branch of the 17th intersegmental artery that accompanies the 15th spinal nerve (Evans, 1909). Dorsoventrally, the 1°SCA lies just ventral to the median plane of the limb (Fig. 2A) and branches distally into a dense capillary network. In the proximal part of the forelimb, however, the artery lies between a ventral and a slightly larger dorsal avascular space. Proximal to these spaces, the artery gives rise to two stereotypic layers of capillaries, one of which passes dorsally and the other ventrally, to encircle these avascular spaces. These dorsal and ventral capillary layers curve toward each other distally to meet the distal branches of the 1°SCA in the dense capillary network described above. There are eventually 4 capillary layers, labeled I–IV, in the D-V plane. The dorsal-most capillary layer at this stage is denoted as capillary layer II, and the ventral capillary layer is denoted as capillary layer IV. The plane of the 1°SCA lies in capillary layer III (Seichert and Rychter 1972a,b). Capillary layer I [see below; E4.5 (HH25)] has not yet formed. These arterial capillaries anastomose throughout the forelimb with capillaries that drain into both the PCV and umbilical veins. These venous capillaries are not restricted to segmental positions (Evans, 1909) in

the A-P axis, but are restricted to one of the same three capillary layers in the D-V axis described above. Peripheral vessels along the postaxial (posterior) border of the forelimb in capillary layer III have begun to form the posterior marginal vein (PMV) (Fig. 2B).

Neurovascular congruence is evident in both the D-V and A-P axes of the forelimb by HH22. There are four (13th–16th) spinal nerves (Bennett *et al.*, 1980) which contribute to the formation of the brachial plexus (Fig. 2B). By HH22, these nerves have begun entering the posterior half of the forelimb (Hollyday, 1995) and converge on the 1°SCA in both the A-P and D-V axes. Peripheral nerves are always found to lie on one of the four capillary layers of the developing forelimb. For example, the brachial plexus lies on the same D-V plane as capillary layer III. The brachial plexus divides into dorsal and ventral nerve sheets that are called brachialis longus superior (BLS) and inferior (BLI), respectively (Hollyday, 1995; Roncali, 1970; Swanson and Lewis, 1982). BLS arches upward avoiding the dorsal avascular space to pass on the dorsal side of capillary layer II. BLI maintains a close spatial relationship to the 1°SCA lying on the ventral side of capillary layer III.

E4.5 (HH25)

The centrally placed 1°SCA is the largest blood vessel in the forelimb (Fig. 2C); however, other (now smaller) segmentally placed DA forelimb vascular branches may still persist (Evans, 1909). In the proximal forelimb, the 1°SCA is now referred to as the brachial artery (BA). The BA divides into median (MA) and supracoracoideus arteries (ScA), both of which lie in the same D-V plane (capillary layer III). The MA is the direct distal extension of the BA, and the ScA is an anteriorly directed branch that demarcates a new avascular space in the A-P axis in which the humerus is formed (Fig. 2C). BLI enters the posterior half of the forelimb and divides into three branches (median, supracoracoideus, and ulnar), two of which track with the aforementioned arteries to form congruent neurovascular entities. The median nerve (Mn) tracks along the ventral surface of the MA, and in the same way that the most distal spinal nerve fibers are those that lie closest to the ISV (see above), the most distally placed fibers of the Mn are those that appear to wrap around the MA (Fig. 2C). The supracoracoideus nerve (Scn) joins the same named artery to form the supracoracoideus neurovascular bundle. The ulnar nerve (Uln) arches along the postaxial border of the forelimb on the ventral surface of capillary layer III, toward the PMV, and in contrast to the other two nerves (which appear to follow the trajectory of their corresponding arteries), foreshadows the trajectory of the ulnar artery (UlA), which has not yet formed.

Vascular remodeling in the posterior part of the forelimb occurs before remodeling in the anterior compartment. For example, the anterior marginal vein (AMV), which is found along the anterior border of the forelimb, forms after the PMV. The PMV enlarges more rapidly than the AMV and joins with it (for they both lie in capillary layer III) to form the marginal sinus (MS) not at the apex but on the preaxial (anterior) border of the forelimb (Seichert and Rychter, 1971, 1972a). The anatomical pattern of peripheral nerves does not change once specific branches have formed within the forelimb. In contrast, the forelimb vascular pattern continues to be remodeled. For example, another avascular space appears dorsal to capillary layer II (Fig. 2D) and ventral to a new discrete layer of capillaries referred to as capillary layer I. Capillary layer I drains into the dorsal body wall venous plexus (Drushel *et al.*, 1985). Proximally, capillary layer II drains into capillary layer III (Fig. 2D), which itself continues to drain into the PCV.

BLS will give rise to the radial nerve (Rn) and both continue to track along capillary layer II. In the same way that the Uln foreshadows the trajectory of the UlA, the Rn foreshadows the trajectory of the profunda brachii artery (PBA), which later forms within capillary layer II.

Nerves in the dorsal half of the limb (e.g., Rn) are always found to lie on the dorsal side of their capillary layer, and nerves in the ventral half (e.g., Mn) always lie on the ventral side of their capillary layer (Fig. 2D). Thus, with respect to the D-V axis of the forelimb, peripheral nerves are always positioned peripheral to their corresponding blood vessels (Fig. 2E).

E5 (HH26)

The distal end of the MA now arches along a postaxially directed curve. The Mn continues to track along the MA on the ventral surface of capillary layer III (Fig. 3A). It follows the trajectory of the MA in the A-P axis as it curves postaxially; however, the Mn lies slightly preaxial to the MA in this plane (Fig. 3B). In the same way that peripheral nerves are always positioned peripheral to their corresponding blood vessels in the D-V axis, they are also positioned peripheral to their corresponding blood vessels in the A-P axis of the forelimb.

Peripheral nerves always maintain a close spatial relationship to the capillary layers along which they track and, furthermore, only cross the avascular spaces between these layers at points where capillary layers merge. For example, in the proximal region of the forelimb, a superficial sheet of dorsal cutaneous nerves branch from the Rn. These nerves travel on the dorsal surface of capillary layer I and only branch from the Rn to traverse the avascular space between capillary layers I and II at precisely the point where these capillary layers merge (Fig. 3C).

In the same way that changes to the vascular pattern occur in the posterior part of the forelimb before the anterior part (e.g., formation of the PMV), extensions to the peripheral nerve pattern also occur asymmetrically over time. Changes in the trajectory of peripheral nerves in the dorsal compartment of the forelimb precede those occurring in the ventral compartment. For example, despite having similar A-P trajectories, the Rn lies distal to the Mn as they enter the forelimb. The Rn gives off a postaxially directed

branch (Fig. 3C) which will form both the axillaris nerve and dorsal cutaneous branches (Hollyday, 1995; Swanson and Lewis, 1982).

In the midportion of the forelimb (future elbow region), capillary layer II curves down toward the BA (capillary layer III) to eventually anastomose with it immediately distal to the humerus in the space between the proximally separated radius and ulna. As the radius and ulnar continue to separate from each other in a proximal-to-distal direction, this anastomosis gradually lengthens distally to form the MA. Distal to the anastomosis, the two joined capillary layers that have formed the MA again diverge by projecting dorsally and ventrally around the distally unseparated radius and ulna (Figs. 3D and 3E). The Mn diverges with the ventral branch and the Rn diverges with the dorsal vascular branch of the MA. All four capillary layers converge again distally into the MS at the apex of the forelimb.

A rudimentary UlA can be seen branching from the BA in the proximal postaxial part of the forelimb, but its form is lost distally as it merges with capillaries in layer III (Fig. 3F). The Uln divides proximally into a cranial branch, which projects toward the MA (Nickel *et al.*, 1977), and a caudal branch, which continues along the PMV. The pectoralis nerve is a ventrally placed branch of BLI that contributes to the formation of the pectoralis neurovascular bundle. This nerve arches craniad and lateral to the forming humerus (Fig. 3F).

There is a close correlation between the stereotypic stratification of neurovascular structures in the D-V axis and three regions of the forelimb: the cartilage forming region, the muscle forming region, and the peripheral avascular zone (Fig. 3G). The cartilage anlagen that will form the humerus, the radius, and the ulna lie within (but do not completely occupy) the space between capillary layers II and III. The dorsal and ventral muscle masses form between capillary layers I and II and III and IV, respectively. There are never any dorsoventrally oriented communicating vessels located between capillary layers II and III other than the convergence of capillary layers II and III to form the MA in the center of the forelimb described above. In contrast, there are occasional dorsoventrally oriented communicating vessels between capillary layers I and II and between III and IV that pass between the muscle masses (e.g., ventrally, between the UlA and capillary layer IV). Capillary layers I and IV lie consistently approximately 100 μm distant from the ectoderm of the entire forelimb (Martin *et al.*, 1989).

E5.5 (HH27–HH28)

There is a hierarchy of neurovascular congruence in the developing forelimb. Neurovascular congruence is always maintained in the D-V plane and is greater than that seen in the A-P plane. For example, the dorsal cutaneous nerves that branch from the Rn (Fig. 4A) are not always accompa-

FIG. 1. (A) Dorsal view of whole mount at HH17 showing segmental (asterisk) and nonsegmental (square) lateral arterial branches of the dorsal aorta (DA) contributing to the formation of the capillary plexus (CP) in the forelimb (FL). Spinal nerves (SN) emerging from the neural tube (NT) occupy the anterior half somite. Leading SN axons (arrowhead) lie closest to the intersomitic vein (ISV) but do not make physical contact with this vessel. The dotted line indicates the plane of section in (B). (B) Sagittal whole-mount section showing the large ISV (bracket) along whose ventral aspect SN appear to track. The DA gives rise to a series of segmental dorsal (ISA) and lateral arterial (asterisk) branches. (C). HH17 whole mount sectioned in a dorsal–oblique plane showing that SN lie dorsal to forelimb capillaries that branch from the DA (asterisk) in the region medial to the PCV. Lateral to the PCV both axons and forelimb capillaries lie in the same D-V plane. (D) Ventral view of a HH21 whole mount sectioned through the dorsal portion of the DA. ISA and the lateral (segmental) forelimb arteries arise from a common arterial trunk (square) at HH21. The lateral forelimb arteries (arrowheads) lie cranial to the ISV. The ISA lie caudal to the ISV. The lateral forelimb artery between the 18th and 19th somites (asterisk) has enlarged to become the largest artery supplying the forelimb and is named the 1° subclavian artery. The SN that contribute to the formation of the brachial plexus (BP) have been numbered accordingly. Figures are oriented with the lateral border to the right and in (A), (C), and (D) anterior (cranial) border uppermost.

FIG. 2. (A) Sagittal whole-mount section showing the close spatial relationship between the brachial plexus (BP) and the 1° subclavian artery (asterisk) in the D-V axis at HH21. The BP divides into a dorsal and ventral branch. The dorsal branch is called brachialis longus superior (BLS), and it tracks along the dorsal surface of capillary layer II. The ventral branch is called brachialis longus inferior (BLI), and it tracks along the ventral surface of capillary layer III. All capillary layers converge distally as a plexus (CP). (B) Dorsal whole mount at HH23 showing the convergence of spinal nerves (numbered 13–16) to form the BP, which lies in the same anteroposterior position as the 1° subclavian artery (asterisk). The posterior marginal vein (PMV) has begun to form along the posterior border of the forelimb. (C) Ventrally viewed HH25 whole mount showing the three divisions of BLI. The supracoracoideus nerve tracks with its artery (ScA) as the supracoracoideus neurovascular bundle (asterisk) and demarcates the avascular humerus (H). The median nerve (Mn) tracks along and around the median artery (MA). Leading axons of the Mn are those which lie closest to the MA. The ulnar nerve (Uln) arches toward the PMV. (D) Sagittal whole-mount section of an HH25 proximal forelimb showing the formation of capillary layer I. The radial nerve (Rn) is always found on the dorsal surface of capillary layer II, and the Mn is always found on layer III. (E) Scheme showing the chief neurovascular relationships that have been established by HH25. Peripheral nerves are always found to lie on one of four discrete capillary layers that are defined by their position in the D-V axis of the developing forelimb. With respect to the median plane of the forelimb, peripheral nerves (green) are always positioned peripheral to their corresponding blood vessels (red) in the D-V axis. For example, nerves in the dorsal half of the limb will lie on the dorsal surface of the capillary layer on which they track, and nerves in the ventral half will lie of the ventral surface of the capillary layer on which they track. All figures are oriented with the lateral border to the right. The cranial border is uppermost in (B), (C), and (E).

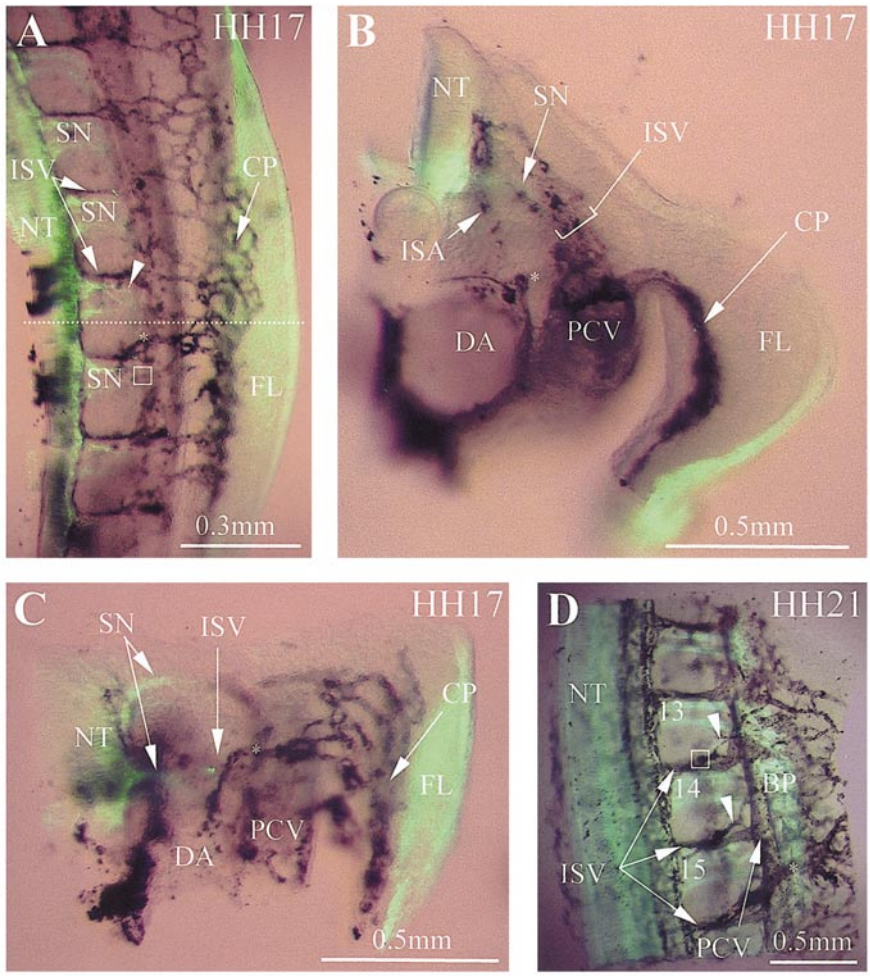

1

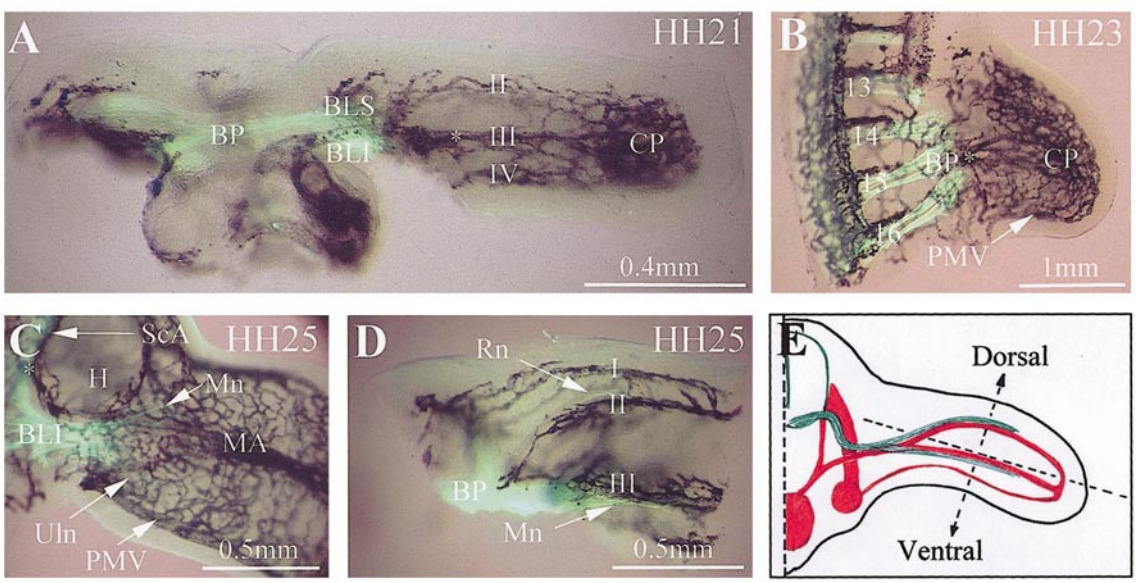

2

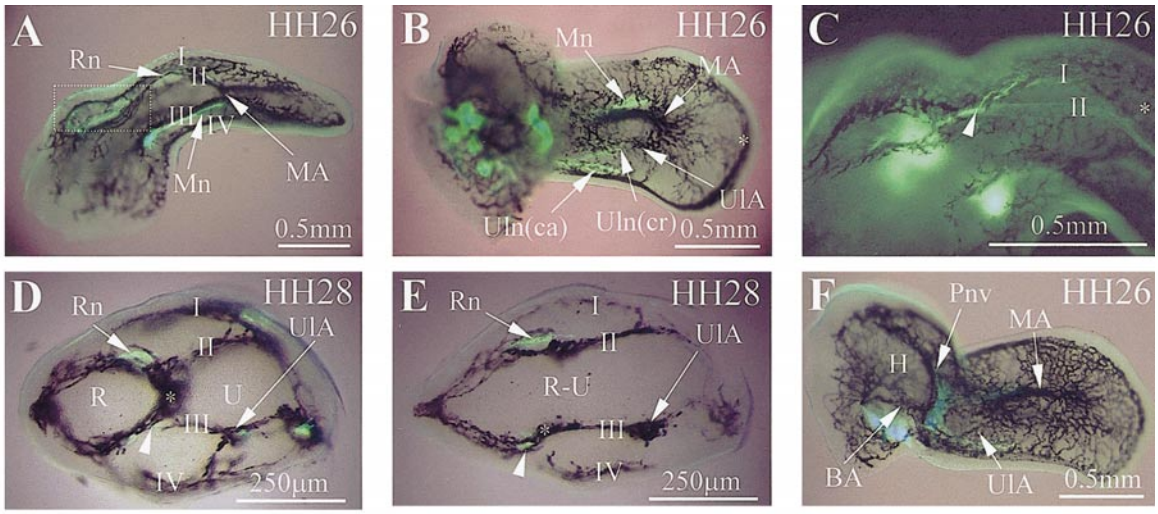

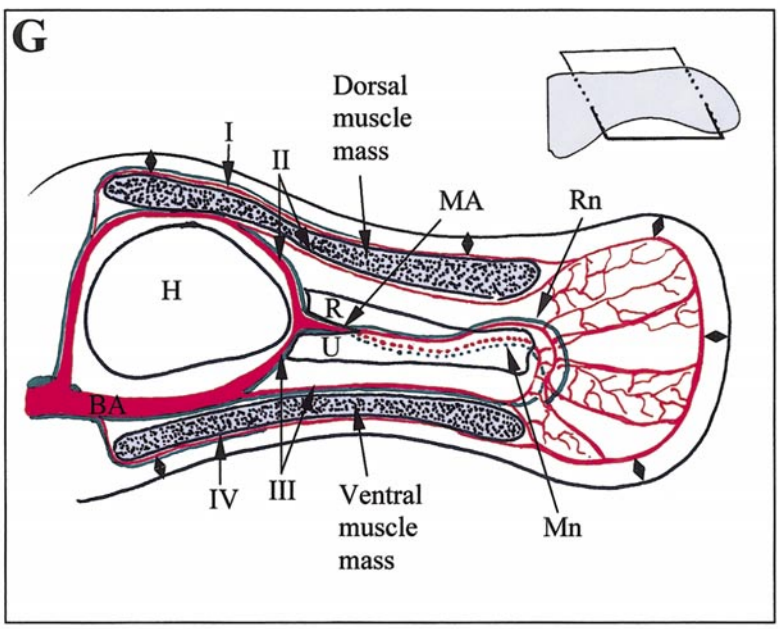

3

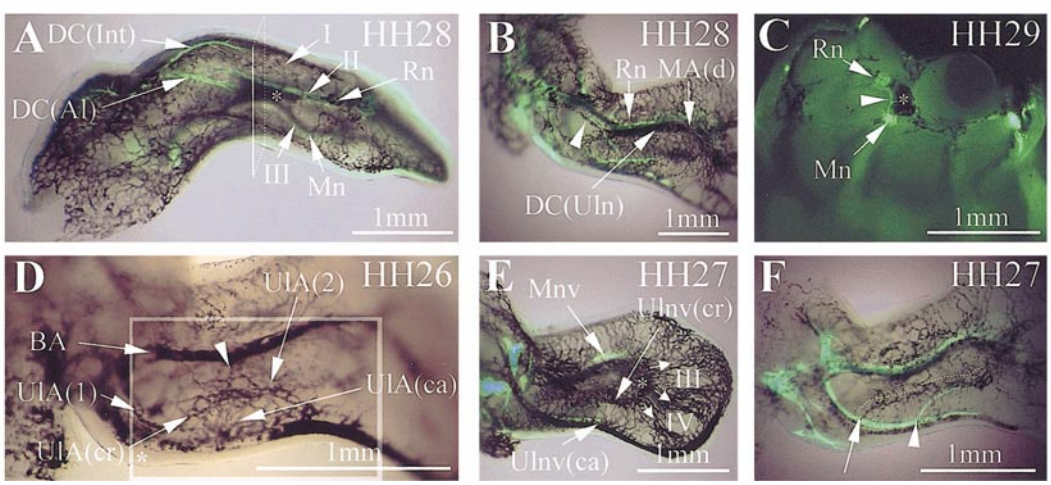

4

nied by discrete vessels in the A-P plane (Martin and Lewis, 1989), but nevertheless always retain their D-V congruence on the dorsal surface of capillary layer I. In contrast to the lack of congruency between cutaneous nerves and blood vessels in capillary layers I and IV (away from the D-V center of the forelimb) in the A-P axis, the Rn and the Mn maintain A-P congruency with the dorsal and ventral branches of the MA, respectively (capillary layers II and III), that lie closer to the D-V center of the forelimb. Neurovascular congruency in the D-V axis does not vary, but congruency in the A-P axis does: A-P congruency is highest toward the center of the forelimb and decreases with increasing distance away from the center. For example, in the proximal forelimb, BLS is not confined to exactly the same A-P trajectory as the PBA (because it has a larger A-P width than the vessel), but both structures are confined to the same D-V position that corresponds to capillary layer II. Further distally (toward the P-D center of the forelimb), the capillaries in layer II are divided by a V-shaped (apex pointing distally) avascular space on the dorsal surface of the humerus. Here, the Rn lies in precisely the same A-P plane as the preaxial border of this V-shaped gap (Fig. 4B). Like all other forelimb nerves, the Rn does not traverse any portion of the forelimb without its capillary layer. Where the MA anastomoses with capillary layer II (see above), the Rn and Mn appear to exchange axons around the MA (Fig. 4C).

In most cases, blood vessels are present in the forelimb before their corresponding peripheral nerves, but there are several exceptions to this rule (e.g. UlA). The UlA is formed in two phases: in the first phase, the primary UlA branches from the proximal portion of the BA [see above, E5 (HH26)] and follows a path parallel and on the cranial side of the PMV. Like the Uln, the primary UlA divides into cranial and caudal branches (Fig. 4D). The P-D location of the cranial branch of the UlA was difficult to define, but in over 470 forelimbs, was always located up to 100 μm distal to the prospective elbow region (Fig. 4D, asterisk). The cranial

FIG. 3. (A) Sagittal whole-mount section at HH26 showing the four capillary layers (labeled I–IV) along which peripheral nerves track. The radial nerve (Rn) tracks along the dorsal surface of capillary layer II, which arches ventrally to anastomose with capillary layer III to form the median artery (MA). Proximal to this anastomosis, the median nerve (Mn) tracks along the ventral surface of the brachial artery. The area enclosed by the dotted box is enlarged in (C). (B) Ventral whole-mount section showing the Mn tracking along the preaxial border of the MA. The cranial branch of the ulnar nerve (Uln(cr)) foreshadows the trajectory of the ulnar artery (UlA). The caudal branch of the ulnar nerve (Uln(ca)) tracks along the posterior marginal vein. The posterior marginal vein joins the anterior marginal vein to form the marginal sinus (asterisk). (C) Sagittal whole-mount section showing that the dorsal cutaneous branches of the radial nerve cross the avascular space between capillary layers I and II only at the point at which these layers merge (arrowhead). The radial nerve gives off a postaxially directed branch (asterisk). (D) Coronal whole-mount section at HH28 of the proximal zeugopod showing the median nerve (arrowhead) lying on the ventral surface of the median artery (asterisk). The radius (R) and the ulna (U) are enclosed by capillary layers II and III, and the dorsal and ventral muscle masses lie between capillary layers I, II, III, and IV, respectively. The median artery forms between the separated R and U. (E) Coronal whole-mount section of the distal zeugopod showing the unseparated radius and ulna (R-U) around which capillary layers II and III diverge. (F) Ventral whole-mount section at HH26 showing the UlA branching from the brachial artery (BA) and the pectoralis neurovascular bundle (Pnv) arching around the lateral border of the humerus (H). (G) Scheme showing the relationship between peripheral nerves (green), blood vessels (red), muscle (stippled), peripheral avascular zone (diamond), and the humerus (H), radius (R), and ulna (U). The oblique plane of the schematic is illustrated by the figure in the top righthand corner. The stereotypic stratification of neurovascular structures into four D-V layers (I–IV) spatially correlates (negatively) with the cartilage, muscle, and the peripheral avascular zone. Figures are oriented with the lateral border to the right and cranial border uppermost. Coronal and sagittal sections are oriented with the dorsal surface uppermost and coronal sections are oriented with the postaxial border to the right.

FIG. 4. (A) Whole mount viewed from the anterior border of the forelimb at HH28 showing that, although the dorsal interosseous cutaneous nerve (DCInt) and the dorsal alar cutaneous nerve (DCAl) may not be congruent with blood vessels in the A-P axis, they are always congruent with blood vessels in the D-V axis (capillary layer I). The radial (Rn) and the median (Mn) nerves are congruent in both the A-P and D-V axes of the forelimb. Neurovascular congruency decreases with increasing distance from the center of the forelimb. The rectangle indicates the plane of the coronal section in (C). (B) Dorsal view of a HH28 whole mount showing the congruent neurovascular border (arrowhead) shared by the Rn and capillaries in layer II on the dorsal surface of the humerus. The Rn tracks with the dorsal branch of the median artery (MA(d)). DC(Uln), Dorsal ulnar cutaneous nerve. (C) Coronal whole-mount section at HH29 showing that the Rn and the Mn exchange axons (arrowhead) around the median artery (asterisk) in the centre of the forelimb. These axons appear to be in intimate physical contact with the artery. (D) Ventrally viewed HH26 whole mount showing the formation of the ulnar artery (UlA) in the area enclosed by the box. The UlA forms in two phases: the primary ulnar artery (UlA(1)) branches from the brachial artery (BA) and divides into a cranial (UlA(cr)) and caudal (UlA(ca)) branch; UlA(cr) then joins a postaxial branch of the BA to form the secondary (definitive) ulnar artery (UlA(2)). Asterisk, prospective elbow. (E) Ventrally viewed HH27 whole mount showing the median neurovascular bundle curving toward the ulnar neurovascular bundle (Ulnv(cr)). The MA and the UlA(2) join to form the ventral carpal arch (asterisk) from which digital arteries project into the autopod (arrows). Avascular spaces appear in a posteroanterior sequence and demarcate the region in which future digits will form (digits numbered IV and III). Ulnv(ca), caudal ulnar neurovascular bundle. (F) Ventrally viewed HH27 wholemount showing that the cranial branch of the Uln (arrowhead) branches distal to the cranial branch of the UlA (arrow). The UlA appears to form by intercalation of adjacent capillaries in layer III, and its trajectory is indicated by the dotted line. Figures are oriented with the lateral border to the right and anterior border uppermost. Coronal sections are oriented with the dorsal surface uppermost and the postaxial border to the right.

branches of the Uln and the UlA curve anteriorly toward the MA; in the second phase of UlA development at HH26, a postaxial branch of the BA joins the capillaries into which the cranial branch of the primary UlA has previously merged (Fig. 4D). These capillaries appear to be undergoing intercalation to form the secondary and definitive UlA. The caudal branch of the Uln maintains a close spatial relationship to the PMV and the caudal branch of the primary UlA. This arterial branch becomes the vasa nevorum to the caudal branch of the Uln (Fig. 4E). The P-D point at which the cranial branch of the Uln branches from the Uln varies; however, it is always distal to the point at which the cranial branch of the primary UlA bifurcates (Fig. 4F).

The dorsal and ventral branches of the MA curve postaxially to form vascular arches in the autopod. The recently formed UlA and the ventral branch of the MA curve toward each other to form the ventral carpal arch (VCA) at HH29 (see below). Likewise, the dorsal branch of the MA curves postaxially, but has not yet anastomosed with the ulnar artery to form the dorsal carpal arch (DCA). From these arches, capillaries project distally to the MS in the apex of the forelimb. In the same way that the PMV forms before the AMV [see above, E4.5 (HH25)], the avascular spaces that appear within these capillaries form in a distinct posteroanterior sequence and demarcate digits IV, III, and II, respectively. The longitudinal capillaries on either side of these avascular spaces will become the future digital arteries.

E6 (HH29)

Peripheral nerves and blood vessels have a preference for certain trajectories in the A-P axis of the developing limb. For example, the Rn and the Mn occupy similar A-P positions despite occupying different D-V levels in the developing forelimb. In the same way that the Mn lies slightly to the preaxial side of the ventral MA branch in the A-P axis, the Rn lies slightly to the preaxial side of the dorsal MA branch (Fig. 5A). The DC Uln (dorsal cutaneous nerve branch on the ulnar side) and the Uln also occupy similar A-P trajectories, despite having different D-V trajectories. Blood vessels occupy a similarly restricted set of A-P trajectories. For example, both the ventral and dorsal branches of the MA lie in the same A-P plane of the forelimb.

Although the Rn and the Mn follow the same D-V and A-P trajectories as the dorsal and ventral MA branches, respectively, the P-D location of their respective curvatures is not always precisely matched (Fig. 5B). At the junction of zeugopod and the autopod, the MA and the UlA unite to form the VCA and the Mn curves postaxially to anastomose with the cranial branch of the Uln. The distal anastomosis between the Mn and the Uln has been described before (Swanson and Lewis, 1982) and is known as the Martin–Gruber anastomosis (Bergman *et al.*, 2001b). In over 200 forelimbs, the Martin–Gruber anastomosis (MG) always occupied the same trajectory as the VCA in the D-V and A-P axes, but was found up to 30 μm distal to the VCA in the P-D axis.

The cranial branch of the Uln lies peripheral (postaxial) to the UlA in the A-P axis. Several small nerves branch between the cranial and caudal parts of the Uln proximal to where the cranial branches of the Uln and UlA are found to lie in the same A-P plane. These small nerve branches do not run parallel with any blood vessels in the A-P or P-D axis, but nevertheless always lie on the ventral surface of capillary layer III (Fig. 5C). Neurovascular congruency in the A-P axis is greater than that observed in the P-D axis, which is the least congruent of the three forelimb axes.

The DC Uln passes dorsally from capillary layer II to capillary layer I, where capillary layers I and II merge laterally. In the autopod, the Rn gives off a cutaneous nerve branch which also reaches capillary layer I where capillary layers I and II merge laterally (Fig. 5D). The dorsal branch of the MA supplies digital arteries between digits II and III, III and IV, and on the postaxial side of digit IV. A diffuse capillary plexus links adjacent digital arteries in the web spaces. The cranial branch of the primary UlA regresses and the secondary UlA is now solely supplied by the postaxial branch of the BA. The secondary UlA (UlA) is initially larger and more discrete distally than proximally, and in contrast to most nerve–blood vessel relationships, it appears to follow the trajectory of the Uln (Fig. 5E). The UlA enlarges slowly to become the largest forelimb artery at E9 (HH35). The dorsal branch of the MA becomes the definitive MA as the ventral branch slowly regresses in size.

The width of the MS decreases in the apex of the forelimb, but the AMV and the PMV still constitute the major pathways of venous drainage. Venous drainage of the autopod and the zeugopod occurs via the dorsal and ventral capillaries in layers I and IV, respectively. The majority of these capillaries drain into the AMV and the PMV, but the remainder continue to drain dorsally into the dorsal body wall venous plexus and ventrally into the umbilical vein. However, at the junction of the zeugopod and the stylopod in the cubital fossa (elbow), the AMV and the PMV pass from the subcutaneous plane into the developing deep brachial vein (Seichert and Rychter, 1971). This vein develops parallel to and on the postaxial side of the brachial artery.

Motor branches of the Rn, Mn, and Uln have already been described in detail (Hollyday, 1995; Lewis *et al.*, 1981; Noakes *et al.*, 1986; Stirling and Summerbell, 1977; Swanson and Lewis, 1982, 1986). They appear in a well-defined sequence and establish the adult pattern by HH31, just before E7 (Swanson and Lewis, 1982). Motor nerves travel in the mixed nerve and abruptly branch off to innervate the appropriate muscles at specific times and positions (Lewis *et al.*, 1981; Swanson and Lewis, 1982). In contrast to the situation in the human adult (Taylor *et al.*, 1994), blood vessels do not consistently accompany motor nerves at these points of initial branching. For example, at the time of initial branching, the motor nerve to the flexor carpi ulnaris

muscle (Fig. 5E) does not have an accompanying blood vessel.

E6.5 (HH30)

Digital branches of the Rn travel on the dorsal surface of their corresponding digital arteries (Fig. 6A). Both arteries and nerves bifurcate at exactly the same position on the dorsal surface of the autopod. Dorsally and on the postaxial border of the autopod there is congruence in the patterning of digital neurovascular bundles in all three axes of the forelimb. In contrast, the digital nerves to digits III and IV, which branch from the MG [see above, E6 (HH29)] pass distally in the midline of their respective digits without an accompanying artery in the A-P axis (Fig. 6A). They do, however, maintain their D-V relationship to capillary layer III.

The Mn gives rise to a branch proximally which curves distally toward the anterior border of the forelimb. This branch divides early into motor and sensory nerves (Fig. 6B). The motor nerve supplies the pronator superficialis muscle (Swanson and Lewis, 1982) and the sensory nerve supplies the patagium (propatagialis nerve) (Nickel *et al.*, 1977). The propatagialis nerve (PGn) precedes and presages the trajectory of the propatagialis artery (PGA) that later accompanies it (Fig. 6C).

E7 (HH32)

The MA remains the largest forelimb artery, and as the limb elongates, the point at which the PBA joins the MA lies further proximally at the level of the cubital fossa (Fig. 6C). The proximal Rn tracks with the PBA, and at the level of the cubital fossa where the PBA joins the MA, the Rn passes to the dorsal surface of the MA. Proximally in the forelimb, BLI passes distally on the ventral surface of the BA and the brachial vein and branches into the Mn and the Uln. The Mn continues distally along the ventral surface of the MA. The Rn and the Mn remain on the dorsal and ventral surfaces of the MA, respectively, to at least E15 (HH41). The Uln branches away from the Mn at the cubital fossa to pass in association with the ulnar vasa nevorum and the PMV to the postaxial border of the forelimb. The Uln(cr) leaves the Uln(ca) proximally in the zeugopod. This branch then traverses the ventral surface of capillary layer III without an accompanying blood vessel to reach the distal portion of the UlA in the distal part of the zeugopod (Fig. 6D).

At E7 (HH32), the ventral branch of the MA has begun to regress (Fig. 6E). The MS also continues to degenerate, and the connections of both the AMV and the PMV with the brachial vein become prominent (Seichert and Rychter, 1971). The AMV and the PMV are now denoted as the cephalic vein and basilic veins, respectively.

E8 (HH34)

We have examined the vascular pattern in 106 E8–E15 (HH34–HH41) forelimbs and have determined that the adult vascular pattern is established by E8. The UlA is now well defined along its entire extent and is the same size as the MA. The UlA branches from the BA at the cubital fossa. With further elongation and rotation of the forelimb, the UlA lies ventral to the MA, which curves dorsally behind it. The UlA still joins the regressing ventral branch of the MA in the VCA. The UlA supplies the digital artery to the postaxial side of digit III and also gives an anterior branch to form the digital artery supplying the ventral surface of digit II. Distal to the VCA, the ventral branch of the MA supplies a digital artery to the preaxial side of digit III and via a branch of this vessel supplies a digital artery to the postaxial border of digit II. A deep branch of the UlA can be seen anastomosing with the MA to form the dorsal carpal arch (Fig. 6E). The caudal branch of the UlA (ulnar vasa nevorum) supplies the digital artery to the postaxial border of digit IV. The regressing ventral branch of the MA also branches to anastomose with the PGA (Fig. 6E). The distal continuation of this preaxial ventral anastomosis with the PGA supplies a digital artery to the preaxial border of digit II. The PGA anastomoses with an extension of the PBA in a T-intersection.

E9–E10 (HH35–HH36)

Although the definitive vascular pattern has been established, differential remodeling events (e.g., changes in the caliber of blood vessels) continue to occur. The UlA is now the largest artery supplying to the forelimb and is joined by the cranial branch of the Uln distally in the forelimb (Fig. 7A). This nerve divides distally to supply digital nerves on either side of digit IV. The Mn supplies branches to the preaxial side of digit III and on either side of digit II. In contrast to the situation at HH30, the ventral digital nerves now run together with arteries (Fig. 7B). The Rn and MA supply dorsal digital neurovascular bundles to both sides of digits II, III, and IV (data not shown). Apart from a wider and more complex ramification of nerves and blood vessels supplying the skin, the basic neurovascular pattern remains unchanged from HH36 to at least HH41.

E15 (HH41)

The congruent neurovascular anatomical pattern that has been established prior to HH41 is maintained to this stage. The various anastomoses between the UlA and MA also remain unchanged. The UlA now has venae comitantes and small diameter nerve fibers coursing over its surface (Fig. 7B). The basilic vein has enlarged, and the long bones have conspicuously vascular medullary canals (data not shown). The feather buds along the postaxial margin of the wing now have a neurovascular supply. Blood vessels and nerves supplying these feather buds travel in the same plane and are conspicuously colocalized in a repeating pattern (Fig. 7C).

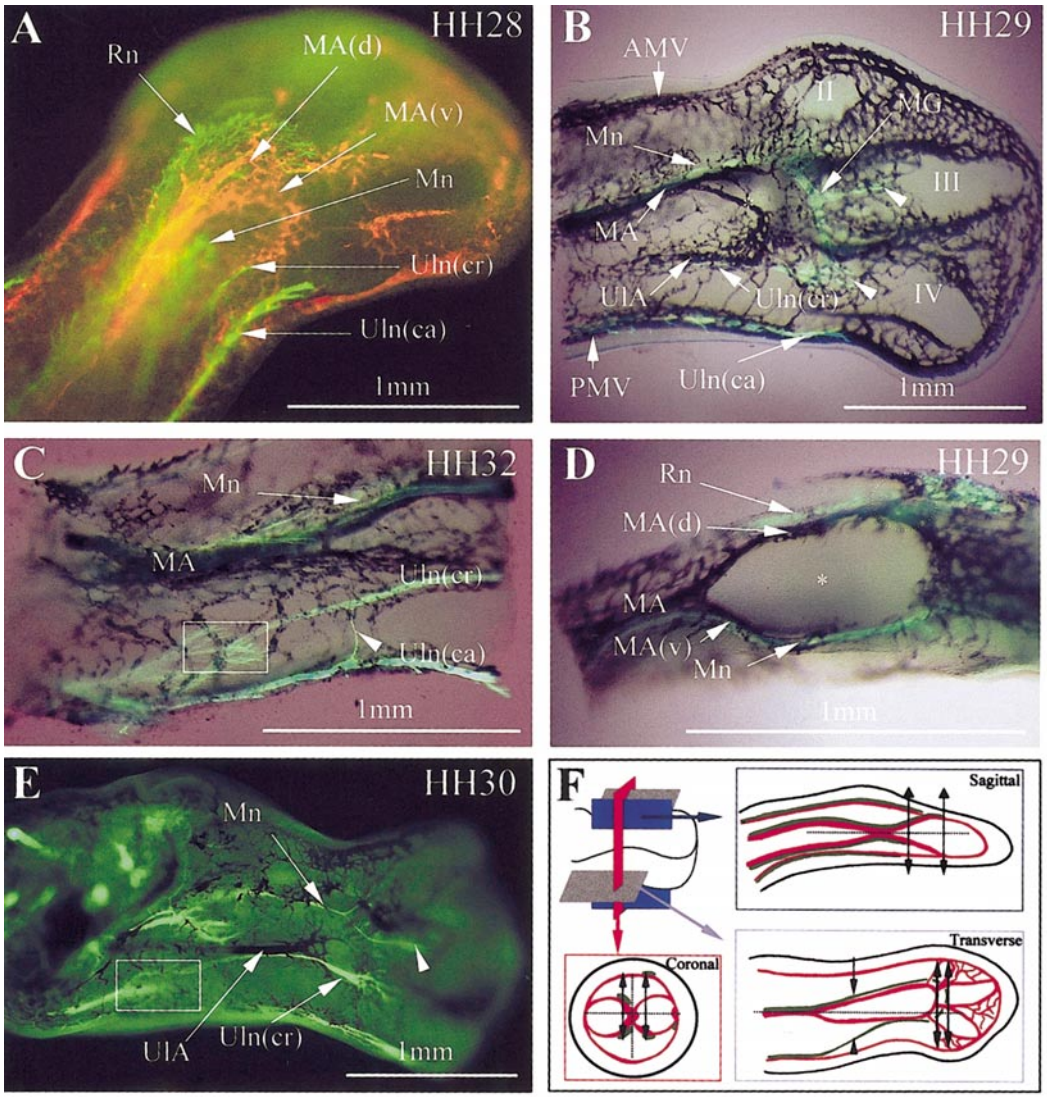

FIG. 5. (A) Dorsal view of a HH28 whole mount showing the parallel trajectories of the radial (Rn) and the median (Mn) nerves that track with the dorsal (MA(d)) and ventral (MA(v)) branches of the median artery, respectively. Like the Rn and the Mn, the cranial (Uln(cr)) and the caudal (Uln(ca)) branches of the ulnar nerve lie peripheral to their corresponding arteries (red). (B) Ventral view of a HH29 whole mount showing the union of the ulnar artery (UlA) with the median artery (MA) to form the ventral carpal arch (asterisk). Similarly, the Mn and the Uln(cr) join to form the Martin–Gruber anastomosis (MG). The MG lies parallel but distal to the ventral carpal arch. Ventral digital nerves (arrowheads) branch from the MG to supply the ventral surface of the digits (II–IV). A digital artery does not initially accompany these nerves in the A-P axis. AMV, anterior marginal vein; PMV, posterior marginal vein. (C) Ventral whole mount (capillary layer IV removed) at HH32 showing a nerve (arrowhead) branching between the Uln(cr) and Uln(ca). The motor nerve to flexor carpi ulnaris (FCU) is not initially accompanied by a blood vessel (box). (D) Sagittally sectioned HH29 whole mount of the distal zeugopod showing the two branches of the MA which diverge to enclose an avascular space (asterisk). The distal dorsal cutaneous branch of the Rn (dotted circle) passes from capillary layer II to layer I at the point where these layers merge laterally. (E) Ventrally viewed HH30 whole mount showing the Uln(cr) foreshadowing the trajectory of the UlA. Box, nerve to FCU; arrowhead, digital nerve. (F) Scheme showing neurovascular spatial relationships in each forelimb axis. Sagittal section (blue), peripheral nerves (green) are always found on one of four capillary (red) layers in the D-V axis. Dorsal peripheral nerves have progressed further distally than ventral nerves (spatial mismatch of double headed arrows); coronal section (red); Peripheral nerves and blood vessels occupy discrete A-P positions in the forelimb at all D-V positions (indicated by path of double headed arrows); transverse section, neurovascular congruency is normally observed in the A-P axis (arrow) but is not invariant (arrowhead). Neurovascular spatial relations are least congruent in the P-D axis (spatial mismatch of double headed arrows). With respect to the central axes of the forelimb (dotted lines in all sections), nerves are always found to lie peripheral to their accompanying blood vessels. Figures are oriented with the lateral border to the right and cranial border uppermost. Sagittal sections are oriented with the dorsal surface uppermost.

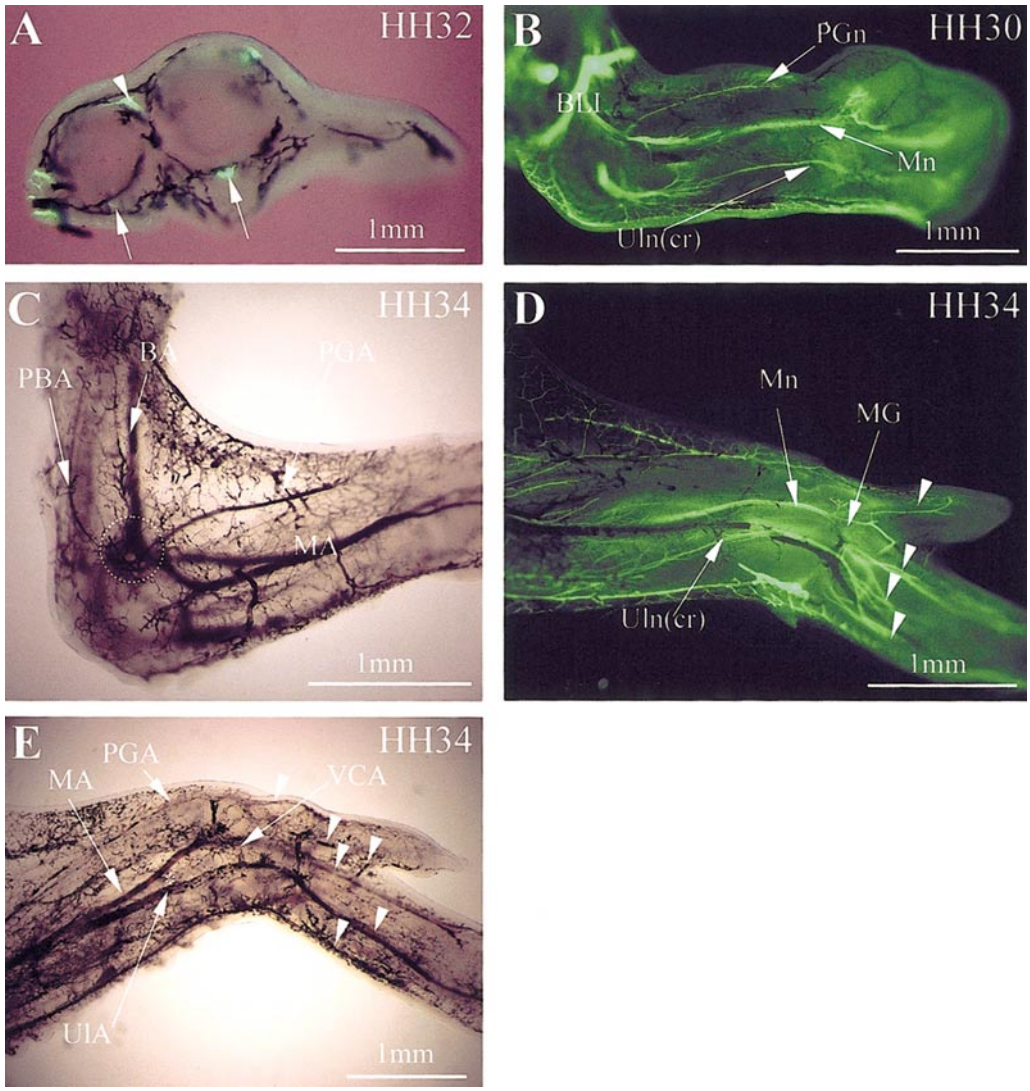

FIG. 6. (A) Coronal whole-mount section at HH32 at the level of the autopod showing dorsal digital nerves (arrowhead) and ventral digital nerves (arrows). (B) Ventrally viewed HH30 whole mount showing the propatagialis nerve (PGn) branching from the median nerve (Mn). The PGn foreshadows the trajectory of the propatagialis artery (PGA) seen in (C). (C) Dorsal view of a HH34 whole mount showing the anastomosis between the profunda brachii artery (PBA) and the PGA (dotted circle). (D) Ventral whole mount at HH34 of distal zeugopod showing how the median nerve (Mn) and the cranial branch of the ulnar nerve (Uln(cr)) join to form the Martin–Gruber neural anastomosis (MG) which supplies ventral digital nerves (arrowheads) to the digits. (E) Ventral view of an HH34 whole mount showing the vascular anastomoses in the distal zeugopod. A rudimentary ventral branch of the MA joins with the UlA to form the ventral carpal arch (VCA). The dorsal branch of the MA joins with the ulnar artery to form the dorsal carpal arch (asterisk). The MA also joins with the PGA (dotted ellipse). These vascular anastomoses supply digital arteries (arrowheads) to the digits. Figures are oriented with the lateral border to the right and anterior border uppermost. Coronal sections are oriented with the dorsal surface uppermost and the postaxial border to the right.

DISCUSSION

Developmental Vascular Anatomy of the Avian Forelimb

The avian forelimb is a valuable model for the study of neurovascular development, but descriptions of the developing vascular pattern after E4.5 (HH25) (Caplan, 1985; Caplan and Koutroupas, 1973; Drushel *et al.*, 1985; Feinberg *et al.*, 1986) have been lacking in detail. This has led to oversimplified and sometimes misinterpreted notions of developmental vascular anatomy in this region.

Drushel *et al.* (1985) state that the precursor to the adult wing vascular pattern has been established by E4.5 (HH25), whereas we find significant differences from the

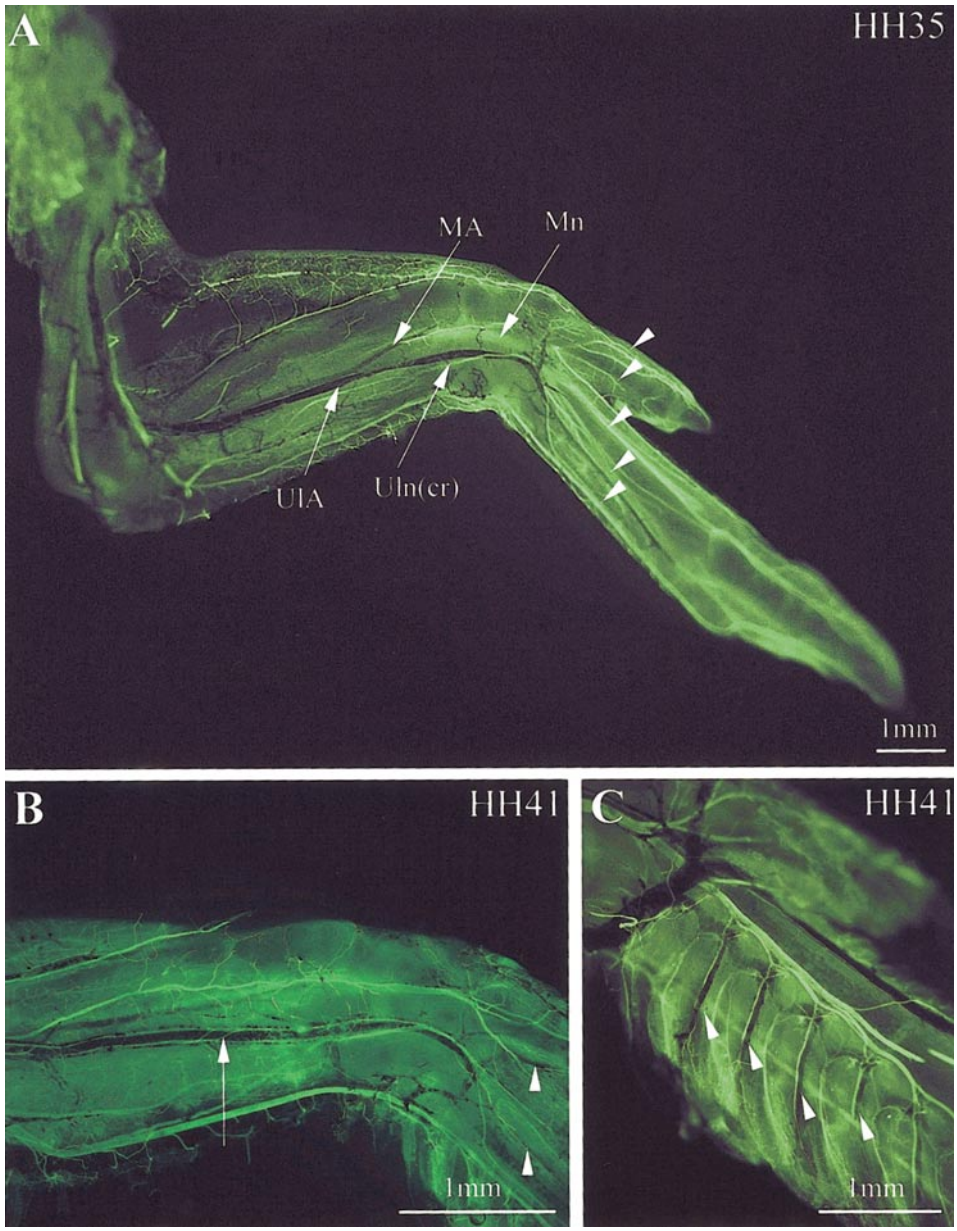

FIG. 7. (A) Ventral aspect at HH35 of a whole mount showing that the ulnar artery (UlA) is now larger than the median artery (MA). The median nerve (Mn) continues to track with the MA and the cranial branch of the ulnar nerve (Uln(cr)) tracks with the UlA. Both the Mn and the Uln contribute digital nerves to the ventral aspect of the digits (arrowheads). (B) Ventral whole mount at HH41 of the distal zeugopod showing small diameter nerve fibers coursing over the surface of the UlA (arrow). The ventral digital nerves (arrowheads) are now spatially associated with digital arteries in the A-P axis. (C) Ventral whole mount of the posterior border of the autopod showing the conspicuously congruent pattern of nerves and blood vessels supplying the featherbuds (arrowheads). Figures are oriented with the lateral border to the right and cranial border uppermost.

adult pattern up to E8 (HH34). These are illustrated schematically in Fig. 8. In particular, we observe the formation of the definitive ulnar artery at E6 (HH29) and both progressive remodeling of the median artery and formation of the propatagialis artery by E8. The propatagialis artery is located on the radial side of the developing forelimb in the quail embryo (Nickel *et al.*, 1977). It has been referred to as the radial artery (Drushel *et al.*, 1985); however, this artery is an anterior branch of the median artery and is accompanied by a branch of the median

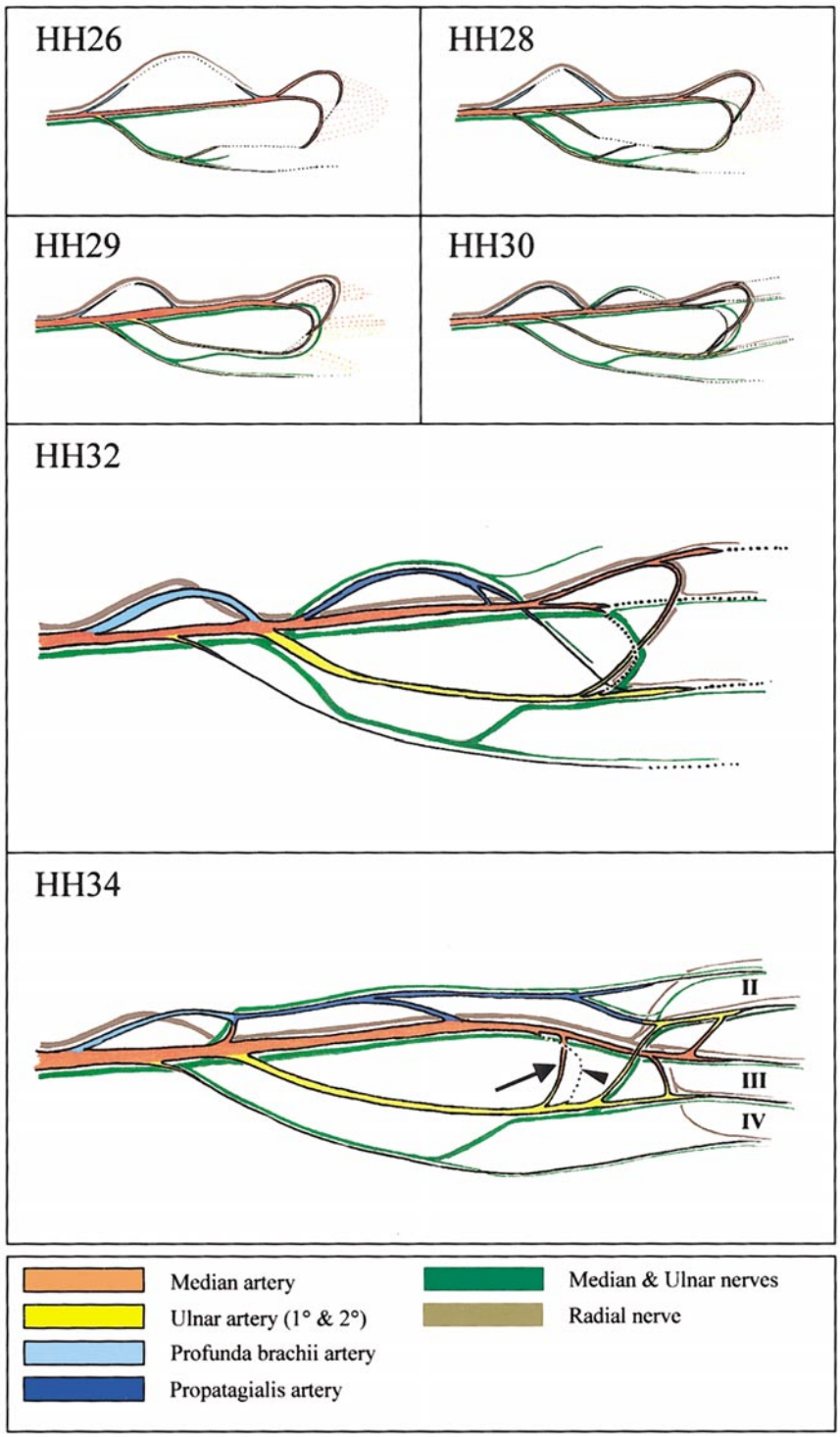

FIG. 8. A series of schematic diagrams that illustrate the critical changes in neurovascular pattern that occur between E5 (HH26) and E8 (HH34). Diagrams emphasize patterns of connectivity in both peripheral nerves and blood vessels and are not drawn to scale. Blood vessels have been outlined with a black line. Capillaries are indicated by a dotted line. Digits are referred to as II (most preaxial), III, and IV (most postaxial). All diagrams are presented as if viewed from the ventral aspect and have been oriented proximal (left); distal (right); anterior (top); posterior (bottom). Peripheral nerves and blood vessels can be identified by referring to the color code at the bottom of the figure. HH26: Capillary layer II anastomoses with the median artery. The radial nerve tracks along capillary layer II, the median nerve tracks along the

nerve called the propatagialis nerve and hence is named accordingly.

The schematic stereogram of the adult vasculature presented by Drushel *et al.* (1985), requires modification: in the E15 (HH41) quail forelimb, there is no radial artery and the radial nerve travels with the median artery, which is present in the quail from E5 (HH26) to at least E15 (HH41; 1 day before hatching). A persistent median artery in the absence of a radial artery is a well-described and relatively common human anatomical variant and is commonly found in other vertebrates (Bergman *et al.*, 2001a). In these anatomical variants, the radial nerve is also found to travel with the median artery. The stereogram of Drushel *et al.* (1985) also indicates that the median artery (called interosseous in their paper) arises from the artery to the ulnar nerve. This blood vessel is actually the cranial branch of the 1° ulnar artery that gives rise to the ulnar artery proper at E5 (HH26) along which the cranial branch of the ulnar nerve tracks. It is the brachial artery that divides to form the median and ulnar arteries. We are confident that the median artery branch of the brachial artery has been correctly named because the median and radial nerves track along it. The anastomosis between the artery supplying the ulnar nerve and the median artery on the dorsum of the forelimb described by Drushel *et al.* (1985) was not observed in our study comprising over 50 perfusions (E8–E15) of this region.

These different descriptions of forelimb vascular anatomy and development could be accounted for by further vascular remodeling after E15, but we feel this is unlikely, as there was no major change in the vascular pattern in 106 forelimbs spanning from E8 to E15. There may also be differences in the adult vascular anatomy between chickens and quails. We also feel this to be unlikely, as our descriptions of the vascular anatomy are consistent with those described in the chicken at earlier stages by Seichert and Rychter (1971, 1972a,b,c) and at adult stages by Nickel *et al.* (1977).

Developmental Peripheral Nerve Anatomy of the Avian Forelimb

In the main, peripheral nerves have been named in accordance with previous studies (Bennett *et al.*, 1980; Hollyday, 1995; Roncali, 1970; Swanson and Lewis, 1982). However, several important anatomical inconsistencies and differences in nomenclature need to be clarified. Roncali (1970) described six spinal nerves (from segments 12 to 17) that contribute to the formation of the brachial plexus in chicken embryos. However, in our study of over 260 quail forelimbs from HH20–H25, we only observed four spinal nerves (from segments 13 to 16) contributing to brachial plexus formation. This is consistent with Bennett *et al.* (1980), but differs from Hollyday (1995), who described a small contribution from the 17th spinal nerve in chicken embryos. These differences could be accounted for by interspecies variability. We have observed axons entering the forelimb at HH22, which is earlier than previously reported (Roncali, 1970; Swanson and Lewis, 1982) but consistent with recent descriptions of forelimb peripheral nerve in-growth (Hollyday, 1995). We have labeled the pectoral nerve in accordance with Hollyday (1995), who described an anteriorly directed nerve branch from BLI in contrast to the posteriorly directed branch described by Roncali (1970) that was not observed in our study. Our description of peripheral nerve development is consistent with the illustrations of Swanson and Lewis (1982). In particular, we have observed a connection between the fibers of the median and ulnar nerves (denoted interosseous and median nerves respectively by Swanson and Lewis, 1982) that has not been described by others (Roncali, 1970) and agree that the adult peripheral nerve pattern is established by HH31. However, we have used different nomenclature to describe the same peripheral nerves to simplify emerging neurovascular spatial relationships. For example, Swanson and Lewis (1982) name the anterior branch of BLI the interosseous nerve and the posterior branch the median nerve. The posterior branch has also been referred to as the median–ulnar nerve (Noakes *et al.*, 1993) and the ulnar nerve (Hollyday, 1995). The anterior branch lies on the ventral aspect of the median artery and supplies motor branches to the ventral muscle mass in the anterior half of the forelimb. It also supplies digital nerves to the ventral autopod. For this reason, we have used *median* to denote the anterior nerve branch of BLI. The posterior branch that has been referred to as both the median–ulnar nerve and the ulnar nerve (see above) divides into a secondary posterior

median artery and the cranial branch of the ulnar nerve lies distal to the cranial branch of the 1° ulnar artery. HH28: Radial and median nerves accompany the dorsal and ventral branches (respectively) of the median artery. The 2° ulnar artery (definitive ulnar artery) has begun to form and the cranial branch of the ulnar nerve foreshadows its trajectory. HH29: The definitive ulnar artery has formed. The ventral carpal vascular arch (union of ulnar artery with ventral branch of median artery) has also formed and is spatially associated with a neural arch that joins the median and ulnar nerves (MG). HH30: The propatagialis nerve (branch of the median nerve) foreshadows the trajectory of the propatagialis artery (branch of the median artery). The dorsal carpal vascular arch (union of ulnar artery with dorsal branch of median artery) has formed and digital neurovascular bundles pass distally between the digits. HH32: The propatagialis artery anastomoses with both the median and ulnar arteries. The ventral carpal vascular arch decreases in size (dotted line). HH34: The definitive neurovascular anatomical pattern is established at this stage. The profunda brachii artery anastomoses with the propatagialis artery. The ulnar artery alters its trajectory in the autopod to supply digital arteries to the digits II and III. The dorsal carpal vascular arch (arrow) and the ventral carpal arch (arrowhead) lie proximal to the origin of these digital arteries.

and secondary anterior branch. The secondary posterior branch has also been referred to as the ulnar nerve (Noakes *et al.*, 1993; Hollyday, 1995) and the secondary anterior branch as the median nerve (Roncali, 1970; Swanson and Lewis, 1982). The secondary posterior nerve branch tracks with a small artery (vasa nevorum) and the posterior marginal vein. It is a sensory nerve (Swanson and Lewis, 1982), and we have referred to it as the caudal branch of the ulnar nerve. The secondary anterior nerve branch lies on the ventral aspect of the ulnar artery and supplies motor branches to the ventral muscle mass in the posterior half of the forelimb. It also supplies digital nerves to the ventral autopod. For this reason, we have used *ulnar* to denote the posterior nerve branch of BLI which divides into cranial (motor) and caudal (sensory) branches. This nomenclature is consistent with the description of avian forelimb anatomy given by Vollmerhaus (Nickel *et al.*, 1977).

The Dynamics of Peripheral Nerve and Blood Vessel Pattern Formation Are Different

Blood vessels. The blood vessel pattern is not static and undergoes a significant change in pattern during the development of the forelimb (Gorski and Walsh, 2001). New branches arise and others regress at specific times and in specific places. The mechanisms responsible for these remodeling events are not known (Beck and D'Amore, 1997); however, the processes of intercalation, intussusception (Carmeliet, 2000; Patan, 1998), and selective apoptosis (Dimmeler and Zeiher, 2000) have been proposed. Those blood vessels that enlarge and persist (e.g., ulnar and median arteries) are spatially associated with major peripheral nerves.

Peripheral nerves. In contrast to the vasculature, the peripheral nerve pattern appears to be established with a high degree of precision *ab initio* (Hollyday, 1990). When a branch is given off, it persists, although fasciculation of these branches occurs progressively with time (Hollyday, 1995). Thus, nerves are normally restricted in their pathways, but under experimental conditions, they can grow anywhere apart from cartilage, the marginal avascular zone, and the region of undifferentiated mesenchyme beneath the apical ectodermal ridge (Swanson, 1985).

Peripheral Nerve and Vascular Patterns Are Largely Congruent in the Developing Avian Forelimb

Our observations of neurovascular development in the forelimb of the avian embryo are in broad agreement with the findings of Martin and Lewis (1989). However, our methods and conclusions differ from theirs and those of a number of other studies (Bennett *et al.*, 1980; Tosney and Landmesser, 1985) in several important respects. Methodologically, by using the entire forelimb from E2–E15 (HH13–HH41) as a model, we have not restricted our analysis to dorsal wing skin preparations (Martin and Lewis, 1989) or serial reconstructions of histological sections (Bennett *et al.*, 1980; Tosney and Landmesser, 1985) at specific and limited time points. Our comprehensive and systematic approach to neurovascular patterning in the whole forelimb has allowed us to document several aspects of neurovascular development that were not apparent in previous studies (see below). In terms of conclusions arrived at, previous studies (Bennett *et al.*, 1980; Martin *et al.*, 1989; Martin and Lewis, 1989; Spence and Poole, 1994; Tosney and Landmesser, 1985) concluded that nerve and blood vessel patterns are, to some extent, random and show no close relationship, whereas we find that neurovascular patterning is highly stereotypic and congruent. However, this relationship is often much more subtle than a strict one-on-one congruency.

In our study of 1636 quail forelimbs aged between E2 and E15 (HH13–HH41), we found that peripheral nerves and blood vessels are always restricted to the same D-V planes. We did not observe any anatomical variants in which this did not occur. Furthermore, peripheral nerves were always found to lie on one of four capillary layers defined by their position in the D-V axis (labeled I–IV in the D-V plane). Peripheral nerves only branched to travel in another D-V plane where capillary layers meet. Subjectively, this creates a strong impression that nerves use these layers as a scaffold along which to track. At no time did we observe peripheral nerves crossing avascular spaces (between capillary layers) without an accompanying blood vessel.

Neurovascular congruency was also observed in the A-P and P-D axes of the developing forelimb; however, there is a hierarchy of congruence between peripheral nerve and blood vessel patterns in the three spatial axes of the forelimb such that D-V congruency>A-P>P-D. The A-P and P-D correlation of peripheral nerve and blood vessel pattern is greatest in capillary layers II and III and decreases with distance from the D-V center of the limb. This resolves the inconsistency between our conclusions emphasizing neurovascular congruency and those of Martin and Lewis (1989), because the latter described the dorsal cutaneous nerves and blood vessels in capillary layer I, where we find least spatial relationships between nerves and blood vessels.

Peripheral nerves and blood vessels were also restricted to specific trajectories in the A-P and P-D axes of the forelimb. For example, DC Uln and the cranial branch of the ulnar nerve lie in the same A-P plane, despite having different D-V coordinates. The radial and the median nerves (and their associated blood vessels) also maintain the same trajectory in the P-D plane, despite having different D-V coordinates. Interestingly, in all cases where nerves and blood vessels were restricted to defined trajectories in each of the three forelimb axes, peripheral nerves were always observed to be positioned spatially peripheral to their corresponding blood vessels (including capillary layers).

The neurovascular pattern is initially symmetrical in all three spatial axes; however, the neurovascular pattern emerges asymmetrically over time (i.e., changes to the

pattern in the dorsal and posterior regions of the forelimb precede those in the ventral and anterior regions). Blood vessels are almost always present before their corresponding nerves (e.g., symmetrical capillary layers along which peripheral nerves subsequently track), although there are several notable reversals of this order: ulnar nerve and artery; propatagialis nerve and artery; ventral nerves to digits III and IV and their arteries.

Potential Mechanisms of Neurovascular Congruence

How the congruence of peripheral nerve and vascular patterns might be achieved can be divided into four broad explanatory groups. The first postulates that the later arriving entity (usually nerves) pattern on the preexisting entity (usually blood vessels), which produce molecular guidance cues, trophic support, or a favorable substrate (Enomoto *et al.*, 2001; Martin and Lewis, 1989; Spence and Poole, 1994). The second suggests that neurovascular congruence can be explained by the two entities sharing the same patterning mechanisms provided by the local nonneural and nonvascular environment (Roush, 1998; Shima and Mailhos, 2000). The third hypothesis suggests that nerves and blood vessels are patterned by different molecular mechanisms that happen to spatially coincide. The fourth postulate is that peripheral nerves and blood vessels are excluded from certain regions by space-occupying structures, such as developing muscle and cartilage, so congruency is achieved by default. This steric exclusion model is not specific in molecular terms, and is thus fundamentally different from receptor–ligand-induced repulsion events that may play a role in schemes two and three.

Tello (1917) proposed the initial version of the first theory and this has since been echoed by others (see above). Consistent with this notion, secretion of the neuroactive factors BDNF, FGF2 and PDGF (Leventhal *et al.*, 1999) by endothelial cells suggests that the vasculature may have a role in supporting neuronal differentiation, survival, and migration. Conversely, it has been proposed that nerves might modify the vasculature pattern (Martin and Lewis, 1989). Trophic factors released by neurons and peripheral nerves, such as VEGF (Ogunshola *et al.*, 2000), dopamine (Basu *et al.*, 2001), CGRP (Haegerstrand *et al.*, 1990), and BDNF (Donovan *et al.*, 1995), have roles in endothelial cell proliferation and migration.

Evidence consistent with the second theory of shared patterning mechanisms is also mounting (Holder and Klein, 1999; Soker, 2001). Molecules that have been found to regulate peripheral nerve development and patterning have also been implicated in the regulation of vascular development and patterning. These molecules include vascular endothelial growth factor (VEGF), neuropilin-1 (NRP-1), semaphorin3A (Sema3A), and the Eph/ephrin and Notch/Delta systems. In addition to VEGF's role as a potent endothelial cell mitogen (Leung *et al.*, 1989), VEGF has also been shown to have multiple neurotrophic effects (Oosthuyse *et al.*, 2001; Schratzberger *et al.*, 2001; Sondell *et al.*, 1999, 2000). VEGF binds to flk-1 (VEGF receptor-2) and NRP1, which are receptors present on nerves and endothelium (Herzog *et al.*, 2001; Kitsukawa *et al.*, 1995; Soker *et al.*, 1998). Moreover, the NRP1 receptor has been recently shown to modulate vasculogenesis (Yamada *et al.*, 2001) and angiogenesis (Soker *et al.*, 1998) in addition to its previously characterized role as a receptor that mediates axonal repulsion and patterning (Fujisawa *et al.*, 1997). Sema3A is another ligand that binds to NRP1 and has been shown to inhibit endothelial cell motility (Miao *et al.*, 1999) in addition to causing growth cone collapse and axonal repulsion (Luo *et al.*, 1993; Raper and Kapfhammer, 1990). Knockout and overexpression studies involving the NRP1/Sema3A system (Behar *et al.*, 1996; Kawasaki *et al.*, 1999; Kitsukawa *et al.*, 1995, 1997; Taniguchi *et al.*, 1997) have demonstrated abnormalities in both peripheral nerve and vascular patterning. Similarly, the Eph/ephrin system has been shown to have a major role in peripheral nerve and vascular patterning (Adams *et al.*, 2001). In particular, the Eph/ephrin system has been shown to have a role in the D-V organization of peripheral nerves (Eberhart *et al.*, 2000; Helmbacher *et al.*, 2000) and A-P patterning of the intersomitic vasculature (Helbling *et al.*, 2000). The Notch/Delta system has also been implicated in axonal guidance (Giniger *et al.*, 1993) and vascular patterning and development (Uyttendaele *et al.*, 2001; Xue *et al.*, 1999).

The third theory holds that neurovascular congruence is established by molecularly different and independent peripheral nerve and blood vessel patterning mechanisms that happen to spatially coincide. For example, expression studies of Slit and Robo reveal patterns that are consistent with a role in axonal guidance and patterning (Vargesson, 2001); however, there is currently no evidence consistent with a similar role for the Slit/Robo system in vascular patterning. Although the Eph/ephrin system has been implicated in both peripheral nerve and vascular patterning, it has not been shown that the same set of Eph/ephrin molecules pattern peripheral nerves and blood vessels in similar ways. Knockout and overexpression studies of putative molecules that simultaneously examine the effect on peripheral nerve and vascular patterning should help resolve whether neurovascular congruence results from shared molecular patterning mechanisms or by different and independent molecular patterning mechanisms that happen to spatially coincide.

The fourth theory offers the simple explanation that the positioning of both nerve and capillary layers is physically determined by the structures that they lie between. This would account for peripheral nerves and capillary layers encircling dense tissues such as cartilage and muscle. Our observation that capillary layers II and III do not abut the cartilage anlagen that they encircle, but instead lie in looser connective tissue at a distance from the cartilage, would argue against this idea. The contributions, which need not be mutually exclusive, of each of these four theories to the

actual development of neurovascular pattern in the forelimb of the quail embryo still remain to be determined.

CONCLUSIONS

We have described the pattern of neurovascular development in the forelimb of the quail embryo in detail and show that the relationship between peripheral nerves and blood vessels is, in the main, highly stereotypic and congruent, rather than being unrelated as suggested by Martin and Lewis (1989). Both the patterns of peripheral nerves and blood vessels appear to be precisely defined. The nature of the cues which define the "highways" (Swanson and Lewis, 1982; Swanson, 1985) along which blood vessels and nerves track remains unresolved (Hollyday, 1995). This more detailed appreciation of neurovascular anatomy and development may hint at which cellular and molecular mechanisms may be responsible and will provide a context within which to interpret experiments that perturb molecular functions.

ACKNOWLEDGMENTS

We thank members of the Embryology Lab, MCRI, particularly Joe Minichiello and Peter Farlie for their valuable input. We are grateful to John Saunders (MBL, Wood's Hole, MA) for his advice on ectoderm removal, Mark Martindale (Kewalo Marine Lab, Honolulu, HI) for suggestions regarding intravascular perfusions with fluorescent dyes, and Heather Robbins (Dept. Anatomy and Cell Biology, University of Melbourne) for confocal microscope instruction and use. The Royal Australasian College of Surgeons, MCRI, Jack Brockhoff Foundation, and the Department of Surgery (Royal Melbourne Hospital, University of Melbourne) generously supported this work. The QH-1 monoclonal antibody developed by F. Dieterlen-Lievre was obtained from the Developmental Studies Hybridoma Bank developed under the auspices of the NICHD and maintained by The University of Iowa, Department of Biological Sciences, Iowa City, IA 52242.

REFERENCES

Adams, R. H., Diella, F., Hennig, S., Helmbacher, F., Deutsch, U., and Klein, R. (2001). The cytoplasmic domain of the ligand ephrinB2 is required for vascular morphogenesis but not cranial neural crest migration. *Cell* **104,** 57–69.

Basu, S., Nagy, J. A., Pal, S., Vasile, E., Eckelhoefer, I. A., Susan Bliss, V., Manseau, E. J., Dasgupta, P. S., Dvorak, H. F., and Mukhopadhyay, D. (2001). The neurotransmitter dopamine inhibits angiogenesis induced by vascular permeability factor/vascular endothelial growth factor. *Nat. Med.* **7,** 569–574.

Beck, L., and D'Amore, P. (1997). Vascular development: Cellular and molecular regulation. *FASEB J.* **11,** 365–373.

Behar, O., Golden, J., Mashimo, H., Schoen, F., and Fishman, M. (1996). Semaphorin III is needed for normal patterning and growth of nerves, bones and heart. *Nature* **383,** 525–528.

Bennett, M. R., Davey, D. F., and Uebel, K. E. (1980). The growth of segmental nerves from the brachial myotomes into the proximal muscles of the chick forelimb during development. *J. Comp. Neurol.* **189,** 335–357.

Bergman, R., Afifi, A., and Miyauchi, R. (2001a). "Illustrated Encyclopedia of Human Anatomic Variation. Opus II: Cardiovascular System: Arteries: Upper Limb, Vol. 2001." Virtual Hospital: University of Iowa Health Care (URL: http://www.vh.org/Providers/Textbooks/AnatomicVariants/Cardiovascular/Text/Arteries/Median.html).

Bergman, R., Afifi, A., and Miyauchi, R. (2001b). "Martin-Gruber Anastomosis, Vol. 2001." Virtual Hospital: University of Iowa Health Care (URL: http://www.vh.org/Providers/Textbooks/AnatomicVariants/NervousSystem/Images/48.html).

Caplan, A. (1985). The vasculature and limb development. *Cell Differ.* **16,** 1–11.

Caplan, A., and Koutroupas, S. (1973). The control of muscle and cartilage development in the chick limb: The role of differential vascularization. *J. Embryol. Exp. Morphol.* **29,** 571–583.

Carmeliet, P. (2000). Mechanisms of angiogenesis and arteriogenesis. *Nat. Med.* **6,** 389–395.

Chaube, S. (1959). On axiation and fate symmetry in transplanted wing of the chick. *J. Exp. Zool.* **140,** 29–77.

Coffin, J., and Poole, T. (1988). Embryonic vascular development: Immunohistochemical identification of the origin and susequent morphogenesis of the major vessel primordia in quail embryos. *Development* **102,** 735–748.

Dimmeler, S., and Zeiher, A. M. (2000). Endothelial cell apoptosis in angiogenesis and vessel regression. *Circ. Res.* **87,** 434–439.

Donovan, M. J., Miranda, R. C., Kraemer, R., McCaffrey, T. A., Tessarollo, L., Mahadeo, D., Sharif, S., Kaplan, D. R., Tsoulfas, P., Parada, L., *et al.* (1995). Neurotrophin and neurotrophin receptors in vascular smooth muscle cells. Regulation of expression in response to injury. *Am. J. Pathol.* **147,** 309–324.

Drushel, R., Pechak, D., and Caplan, A. (1985). The anatomy, ultrastructure and fluid dynamics of the developing vasculature of the embryonic chick wing bud. *Cell Differ.* **16,** 13–28.

Eberhart, J., Swartz, M., Koblar, S. A., Pasquale, E. B., Tanaka, H., and Krull, C. E. (2000). Expression of EphA4, ephrin-A2 and ephrin-A5 during axon outgrowth to the hindlimb indicates potential roles in pathfinding. *Dev. Neurosci.* **22,** 237–250.

Enomoto, H., Crawford, P. A., Gorodinsky, A., Heuckeroth, R. O., Johnson, E. M., Jr., and Milbrandt, J. (2001). RET signaling is essential for migration, axonal growth and axon guidance of developing sympathetic neurons. *Development* **128,** 3963–3974.

Evans, H. (1909). On the earliest blood-vessels in the anterior limb buds of birds and their relation to the primary subclavian artery. *Am. J. Anat.* **9,** 281–319.

Feinberg, R. N., Latker, C. H., and Beebe, D. C. (1986). Localised vascular regression during limb morphogenesis in the chicken embryo. I. Spatial and temporal changes in vascular pattern. *Anat. Rec.* **214,** 405–409.

Flamme, I., Vonreuten, M., Drexler, H., Syedali, S., and Risau, W. (1995). Overexpression of vascular endothelial growth factor in the avian embryo induces hypervascularization and increased vascular permeability without alterations of embryonic pattern formation. *Dev. Biol.* **171,** 399–414.

Fujisawa, H., Kitsukawa, T., Kawakami, A., Takagi, S., Shimizu, M., and Hirata, T. (1997). Roles of a neuronal cell-surface molecule, neuropilin, in nerve fiber fasciculation and guidance. *Cell Tissue Res.* **290,** 465–470.

Giniger, E., Jan, L. Y., and Jan, Y. N. (1993). Specifying the path of the intersegmental nerve of the Drosophila embryo: A role for Delta and Notch. *Development* **117,** 431–440.

Gorski, D. H., and Walsh, K. (2001). Control of vascular cell differentiation by homeobox transcription factors. *Circ. Res.* **88,** 7–8.

Gu, X. H., Terenghi, G., Kangesu, T., Navsaria, H. A., Springall, D. R., Leigh, I. M., Green, C. J., and Polak, J. M. (1995). Regeneration pattern of blood vessels and nerves in cultured keratinocyte grafts assessed by confocal laser scanning microscopy. *Br. J. Dermatol.* **132,** 376–383.

Gu, X. H., Terenghi, G., Purkis, P. E., Price, D. A., Leigh, I. M., and Polak, J. M. (1994). Morphological changes of neural and vascular peptides in human skin suction blister injury. *J. Pathol.* **172,** 61–72.

Haegerstrand, A., Dalsgaard, C. J., Jonzon, B., Larsson, O., and Nilsson, J. (1990). Calcitonin gene-related peptide stimulates proliferation of human endothelial cells. *Proc. Natl. Acad. Sci. USA* **87,** 3299–3303.

Hamburger, V., and Hamilton, H. (1951). A series of normal stages in the development of the chick embryo. *J. Morphol.* **88,** 49–92.

Helbling, P. M., Saulnier, D. M. E., and Brandli, A. W. (2000). The receptor tyrosine kinase EphB4 and ephrin-B ligands restrict angiogenic growth of embryonic veins in *Xenopus laevis*. *Development* **127,** 269–278.

Helmbacher, F., Schneider-Maunoury, S., Topilko, P., Tiret, L., and Charnay, P. (2000). Targeting of the EphA4 tyrosine kinase receptor affects dorsal/ventral pathfinding of limb motor axons. *Development* **127,** 3313–3324.

Herzog, Y., Kalcheim, C., Kahane, N., Reshef, R., and Neufeld, G. (2001). Differential expression of neuropilin-1 and neuropilin-2 in arteries and veins. *Mech. Dev.* **109,** 115–119.

Hobson, M. I., Brown, R., Green, C. J., and Terenghi, G. (1997). Inter-relationships between angiogenesis and nerve regeneration: a histochemical study. *Br. J. Plast. Surg.* **50,** 125–131.

Hobson, M. I., Green, C. J., and Terenghi, G. (2000). VEGF enhances intraneural angiogenesis and improves nerve regeneration after axotomy. *J. Anat.* **197,** 591–605.

Holder, N., and Klein, R. (1999). Eph receptors and ephrins: Effectors of morphogenesis. *Development* **126,** 2033–2044.

Hollyday, M. (1983). Development of motor innervation of chick limbs. *Prog. Clin. Biol. Res.* **110,** 183–193.

Hollyday, M. (1990). Specificity of initial axonal projections to embryonic chick wing. *J. Comp. Neurol.* **302,** 589–602.

Hollyday, M. (1995). Chick wing innervation. I. Time course of innervation and early differentiation of the peripheral nerve pattern. *J. Comp. Neurol.* **357,** 242–253.

Jang, Y. C., Isik, F. F., and Gibran, N. S. (2000). Nerve distribution in hemangiomas depends on the proliferative state of the microvasculature. *J. Surg. Res.* **93,** 144–148.

Kangesu, T., Manek, S., Terenghi, G., Gu, X. H., Navsaria, H. A., Polak, J. M., Green, C. J., and Leigh, I. M. (1998). Nerve and blood vessel growth in response to grafted dermis and cultured keratinocytes. *Plast. Reconstr. Surg.* **101,** 1029–1038.

Kawasaki, T., Kitsukawa, T., Bekku, Y., Matsuda, Y., Sanbo, M., Yagi, T., and Fujisawa, H. (1999). A requirement for neuropilin-1 in embryonic vessel formation. *Development* **126,** 4895–4902.

Keynes, R., and Stern, C. (1984). Segmentation in the vertebrate nervous system. *Nature* **310,** 786–789.

Kitsukawa, T., Shimizu, M., Sanbo, M., Hirata, T., Taniguchi, M., Bekku, Y., Yagi, T., and Fujisawa, H. (1997). Neuropilin-semaphorin III/D-mediated chemorepulsive signals play a crucial role in peripheral nerve projection in mice. *Neuron* **19,** 995–1005.

Kitsukawa, T., Shimono, A., Kawakami, A., Kondoh, H., and Fujisawa, H. (1995). Overexpresion of a membrane protein, neuropilin, in chimeric mice causes abnormalities in the cardiovascular system, nervous system and limbs. *Development* **121,** 4309–4318.

Leung, D., Cachianes, G., Kuang, W., Goedell, D., and Ferrara, N. (1989). Vascular endothelial growth factor is a secreted angiogenic mitogen. *Science* **246,** 1306–1309.

Leventhal, C., Rafii, S., Rafii, D., Shahar, A., and Goldman, S. A. (1999). Endothelial trophic support of neuronal production and recruitment from the adult mammalian subependyma. *Mol. Cell. Neurosci.* **13,** 450–464.

Lewis, J., Chevallier, A., Kieny, M., and Wolpert, L. (1981). Muscle nerve branches do not develop in chick wings devoid of muscle. *J. Embryol. Exp. Morphol.* **64,** 211–232.

Luo, Y. L., Raible, D., and Raper, J. A. (1993). Collapsin: A protein in brain that induces the collapse and paralysis of neuronal growth cones. *Cell* **75,** 217–227.

Manek, S., Terenghi, G., Shurey, C., Nishikawa, H., Green, C. J., and Polak, J. M. (1993). Neovascularisation precedes neural changes in the rat groin skin flap following denervation: An immunohistochemical study. *Br. J. Plast. Surg.* **46,** 48–55.

Martin, P., Khan, A., and Lewis, J. (1989). Cutaneous nerves of the embryonic chick wing do not develop in regions denuded of ectoderm. *Development* **106,** 335–346.

Martin, P., and Lewis, J. (1989). Origins of the neurovascular bundle: Interactions between developing nerves and blood vessels in embryonic chick skin. *Int. J. Dev. Biol.* **33,** 379–387.

Miao, H. Q., Soker, S., Feiner, L., Alonso, J. L., Raper, J. A., and Klagsbrun, M. (1999). Neuropilin-1 mediates collapsin-1/semaphorin III inhibition of endothelial cell motility: Functional competition of collapsin-1 and vascular endothelial growth factor-165. *J. Cell Biol.* **146,** 233–241.

Nickel, R., Schummer, A., and Seiferle, E. (1977). Anatomy of the domestic birds. In "Plates IV and V (Topography of the blood vessels and nerves of the thorax and right wing; after Vollmerhaus—unpublished work carried out at the Institute of Veterinary Anatomy, Giessen)" (W. Siller and P. Wight, Eds.). Verlag, Berlin.

Noakes, P., Hornbruch, A., and Wolpert, L. (1993). The relationship between migrating neural crest cells and growing limb nerves in the developing chick forelimb. In "Limb Development and Regeneration," pp. 381–390. Wiley-Liss, New York.

Noakes, P. G., Everett, A. W., and Bennett, M. R. (1986). The growth of muscle nerves in relation to the formation of primary myotubes in the developing chick forelimb. *J. Comp. Neurol.* **248,** 245–256.

Ogunshola, O. O., Stewart, W. B., Mihalcik, V., Solli, T., Madri, J. A., and Ment, L. R. (2000). Neuronal VEGF expression correlates with angiogenesis in postnatal developing rat brain. *Brain Res. Dev. Brain Res.* **119,** 139–153.

Oosthuyse, B., Moons, L., Storkebaum, E., Beck, H., Nuyens, D., Brusselmans, K., Van Dorpe, J., Hellings, P., Gorselink, M., Heymans, S., Theilmeier, G., Dewerchin, M., Laudenbach, V., Vermylen, P., Raat, H., Acker, T., Vleminckx, V., Van Den Bosch, L., Cashman, N., Fujisawa, H., Drost, M. R., Sciot, R., Bruyninckx, F., Hicklin, D. J., Ince, C., Gressens, P., Lupu, F., Plate, K. H., Robberecht, W., Herbert, J. M., Collen, D., and Carmeliet, P. (2001). Deletion of the hypoxia-response element in the vascular endothelial growth factor promoter causes motor neuron degeneration. *Nat. Genet.* **28,** 131–138.

Patan, S. (1998). TIE1 and TIE2 receptor tyrosine kinases inversely regulate embryonic angiogenesis by the mechanism of intussusceptive microvascular growth. *Microvasc. Res.* **56,** 1–21.

Peng, J., Zhang, L., Drysdale, L., and Fong, G. H. (2000). The transcription factor EPAS-1/hypoxia-inducible factor 2alpha

plays an important role in vascular remodeling. *Proc. Natl. Acad. Sci. USA* **97,** 8386–8391.

Piatt, J. (1942). Transplantation of aneurogenic forelimbs in *Amblystoma punctata*. *J. Exp. Zool.* **91,** 79–101.

Ramer, M., Priestley, J., and McMahon, S. (2000). Functional regeneration of sensory axons into the adult spinal cord. *Nature* **403,** 312–316.

Raper, J. A., and Kapfhammer, J. P. (1990). The enrichment of a neuronal growth cone collapsing activity from embryonic chick brain. *Neuron* **4,** 21–29.

Roncali, L. (1970). The brachial plexus and the wing nerve pattern during early developmental phases in chicken embryos. *Monitore Zool. Ital.* **4,** 81–98.

Roush, W. (1998). Receptor links blood vessels, axons. *Science* **279,** 2042.

Schratzberger, P., Walter, D. H., Rittig, K., Bahlmann, F. H., Pola, R., Curry, C., Silver, M., Krainin, J. G., Weinberg, D. H., Ropper, A. H., and Isner, J. M. (2001). Reversal of experimental diabetic neuropathy by VEGF gene transfer. *J. Clin. Invest.* **107,** 1083–1092.

Seichert, V., and Rychter, Z. (1971). Vascularization of the developing anterior limb of the chick embryo. I. Sinus marginalis: Its development, fate and importance. *Folia Morphol.* **19,** 367–377.

Seichert, V., and Rychter, Z. (1972a). Relationship of the developing vascular bed to morphological differentiation of the wing in the chick embryo. *Folia Morphol.* **20,** 126–129.

Seichert, V., and Rychter, Z. (1972b). Vascularization of developing anterior limb of the chick embryo. II. Differentiation of vascular bed and its significance for the location of morphogenetic processes inside the limb bud. *Folia Morphol.* **20,** 352–361.

Seichert, V., and Rychter, Z. (1972c). Vascularization of the developing anterior limb of the chick embryo. III. Developmental changes in the perimetacarpal capillary network. *Folia Morphol.* **20,** 397–405.

Shima, D. T., and Mailhos, C. (2000). Vascular developmental biology: getting nervous. *Curr. Opin. Genet. Dev.* **10,** 536–542.

Soker, S. (2001). Neuropilin in the midst of cell migration and retraction. *Int. J. Biochem. Cell Biol.* **33,** 433–437.

Soker, S., Takashima, S., Miao, H., Neufeld, G., and Klagsbrun, M. (1998). Neuropilin-1 is expressed by endothelial and tumor cells as an isoform-specific receptor for vascular endothelial growth factor. *Cell* **92,** 735–745.

Sondell, M., Lundborg, G., and Kanje, M. (1999). Vascular endothelial growth factor has neurotrophic activity and stimulates axonal outgrowth, enhancing cell survival and Schwann cell proliferation in the peripheral nervous system. *J. Neurosci.* **19,** 5731–5740.

Sondell, M., Sundler, F., and Kanje, M. (2000). Vascular endothelial growth factor is a neurotrophic factor which stimulates axonal outgrowth through the flk-1 receptor. *Eur. J. Neurosci.* **12,** 4243–4254.

Spence, S., and Poole, T. (1994). Developing blood vessels and associated extracellular matrix as substrates for neural crest migration in Japanese quail, *Coturnic coturnix japonica*. *Int. J. Dev. Biol.* **38,** 85–98.

Stirling, R. V., and Summerbell, D. (1977). The development of functional innervation in the chick wing-bud following truncations and deletions of the proximal–distal axis. *J. Embryol. Exp. Morphol.* **41,** 189–207.

Swanson, G., and Lewis, J. (1982). The timetable of innervation and its control in the chick wing bud. *J. Embryol. Exp. Morphol.* **71,** 121–137.

Swanson, G. J. (1985). Paths taken sensory nerve fibres in aneural chick wing buds. *J. Embryol. Exp. Morphol.* **86,** 109–124.

Swanson, G. J., and Lewis, J. (1986). Sensory nerve routes in chick wing buds deprived of motor innervation. *J. Embryol. Exp. Morphol.* **95,** 37–52.

Tabata, Y. (2001). Recent progress in tissue engineering. *Drug Discov. Today* **6,** 483–487.

Tabin, C. J. (1991). Retinoids, homeoboxes, and growth factors: Toward molecular models for limb development. *Cell* **66,** 199–217.

Taniguchi, M., Yuasa, S., Fujisawa, H., Naruse, I., Saga, S., Mishina, M., and Yagi, T. (1997). Disruption of semaphorinIII/D gene causes severe abnormality in peripheral nerve projection. *Neuron* **19,** 519–530.

Taylor, G., Bates, D., and Newgreen, D. (2001). The developing neurovascular anatomy of the embryo: A technique of simultaneous evaluation using fluorescent labeling, confocal microscopy and three-dimensional reconstruction. *Plast. Reconstr. Surg.* **108,** 597–604.

Taylor, G., Gianoutsos, M., and Morris, S. (1994). The neurovascular territories of the skin and muscles: Anatomic study and clinical implications. *Plast. Reconstr. Surg.* **94,** 1–36.

Teillet, M. A., and Le Douarin, N. M. (1983). Consequences of neural tube and notochord excision on the development of the peripheral nervous system in the chick embryo. *Dev. Biol.* **98,** 192–211.

Tello, J. (1917). Genesis de las teminaxioned nerviosas motrices y sensitivas. *Trab. Lab. Invest. Biol. Univ. Madr.* **15,** 101–199. (cited in Bennett, M. R., Davey, D. F., and Uebel, K. E. (1980). The growth of segmental nerves from the brachial myotomes into the proximal muscles of the chick forelimb during development. *J. Comp. Neurol.* **189,** 335–357.)

Tickle, C. (1991). Retinoic acid and chick limb bud development. *Dev. Suppl.* **1,** 113–121.

Tosney, K. W., and Landmesser, L. T. (1985). Development of the major pathways for neurite outgrowth in the chick hindlimb. *Dev. Biol.* **109,** 193–214.

Uyttendaele, H., Ho, J., Rossant, J., and Kitajewski, J. (2001). Vascular patterning defects associated with expression of activated Notch4 in embryonic endothelium. *Proc. Natl. Acad. Sci. USA* **98,** 5643–5648.

Vargesson, N., Luria, V., Messina, I., Erskine, L., and Laufer, E. (2001). Expression patterns of Slit and Robo family members during vertebrate limb development. *Mech. Dev.* **106,** 175–180.

Waris, T. (1978a). Innervation of scar tissue in the skin of the rat. *Scand. J. Plast. Reconstr. Surg.* **12,** 173–180.

Waris, T. (1978b). Reinnervation of free skin autografts in the rat. *Scand. J. Plast. Reconstr. Surg.* **12,** 85–93.

Weaver, M., and Hogan, B. (2001). Powerful ideas driven by simple tools: lessons from experimental embryology. *Nat. Cell Biol.* **3,** E165–E167.

Xue, Y., Gao, X., Lindsell, C. E., Norton, C. R., Chang, B., Hicks, C., Gendron-Maguire, M., Rand, E. B., Weinmaster, G., and Gridley, T. (1999). Embryonic lethality and vascular defects in mice lacking the Notch ligand Jagged1. *Hum. Mol. Genet.* **8,** 723–730.

Yamada, Y., Takakura, N., Yasue, H., Ogawa, H., Fujisawa, H., and Suda, T. (2001). Exogenous clustered neuropilin 1 enhances vasculogenesis and angiogenesis. *Blood* **97,** 1671–1678.

Received for publication February 4, 2002
Revised June 27, 2002
Accepted June 27, 2002
Published online August 19, 2002